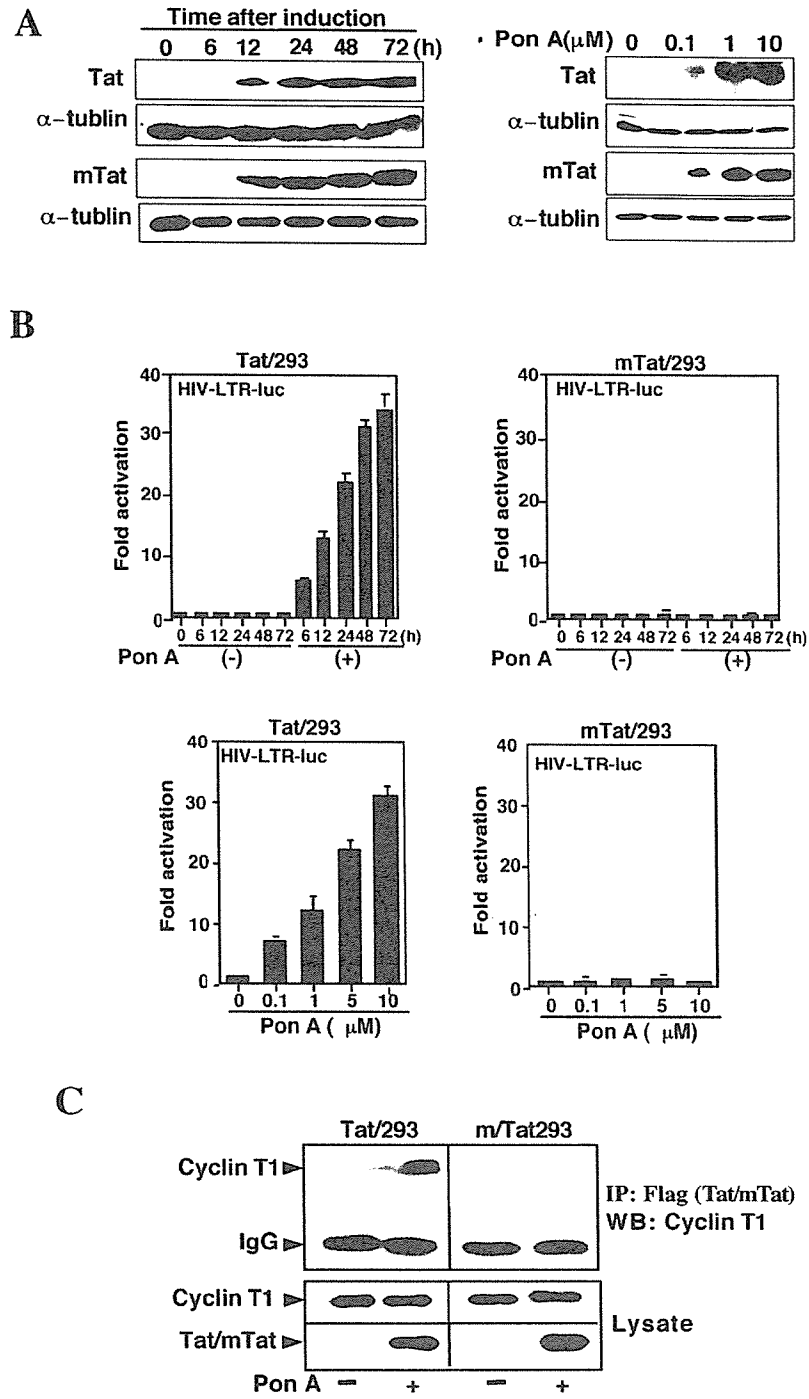

FIG. 1. **Ecdysone-inducible cell lines expressing Tat and mTat.** *A*, inducible expression of Tat and mTat. Tat/293 and mTat/293 cells were treated with PonA (10 μM) for the indicated periods of time (*left panels*) at the indicated concentrations (*right panels*). The FLAG-tagged Tat and mTat proteins were detected by Western blotting with anti-FLAG antibody. Anti-α-tubulin antibody was used to indicate that the equivalent amount of protein from each cell lysate was loaded. *B*, Tat-mediated transactivation of HIV-1 gene expression. Tat/293 (*left panels*) and mTat/293 (*right panels*) cells were transfected with HIV-1 long terminal repeat (*LTR*)-luciferase (*luc*), maintained in culture for 24 h, and then treated for the indicated periods of time with 10 μM PonA (*upper panels*) or for 48 h with various concentrations of PonA (*lower panels*). *C*, co-immunoprecipitation of cyclin T1 with Tat. Tat/293 and mTat/293 cells were treated with PonA for 24 h, and the cell lysates were immunoprecipitated (*IP*) with anti-FLAG antibody (detecting Tat). Immune complexes were collected and subjected to SDS-PAGE, followed by Western blotting (*WB*) with anti-cyclin T1 antibody. One-tenth of each protein lysate used in each reaction was loaded as the input control.

Induction of OGG1 Expression Is Not through the Oxidative Stress Induced by Tat—Because Tat is known to induce oxidative stress (12, 15, 17), it is possible that *OGG1* induction might be an indirect effect of Tat, although it is not yet known whether oxidative stress induces *OGG1* gene expression. We first examined whether Tat induces oxidative stress in Tat/293 cells. Fluorescence-activated cell sorter analysis with the oxidation-sensitive fluorescent probe 2′,7′-dichlorofluorescein diacetate showed that Tat (but not mTat) increased the intracellular ROS levels (Fig. 4*A*). We measured the intracellular levels of GSH and GSSG. As expected, the content of GSSG, the oxidized form of GSH, was increased (~2.3-fold) in Tat-expressing cells in contrast to control mTat-expressing cells (Fig. 4*B*). The GSH (reduced form) level in Tat-expressing cells was decreased to 57% of that in control cells. No significant reduction in GSH was detected in mTat-expressing cells. Furthermore, the manganese superoxide dismutase activity was down-regulated by Tat as reported previously (12). After 24 h of Tat induction, the manganese superoxide dismutase activity was decreased to 59% (Fig. 4*C*).

These results led us to examine whether Tat-induced *OGG1* gene expression is attributable to the oxidative stress associated with Tat action. However, treatment with antioxidants did not block Tat-mediated *OGG1* induction (Fig. 4*D*). 293/Tat cells were pretreated with antioxidants, including pyrrolidine dithiocarbamate, *N*-acetyl-L-cysteine, epigallocatechin gallate (a phenolic antioxidant), and Trolox (a water-soluble vitamin E analog), prior to Tat induction (Fig. 4*D*, *left panel*). When the *OGG1* mRNA was measured by real-time RT-PCR, Tat-induced *OGG1* expression was not affected by the antioxidants. In

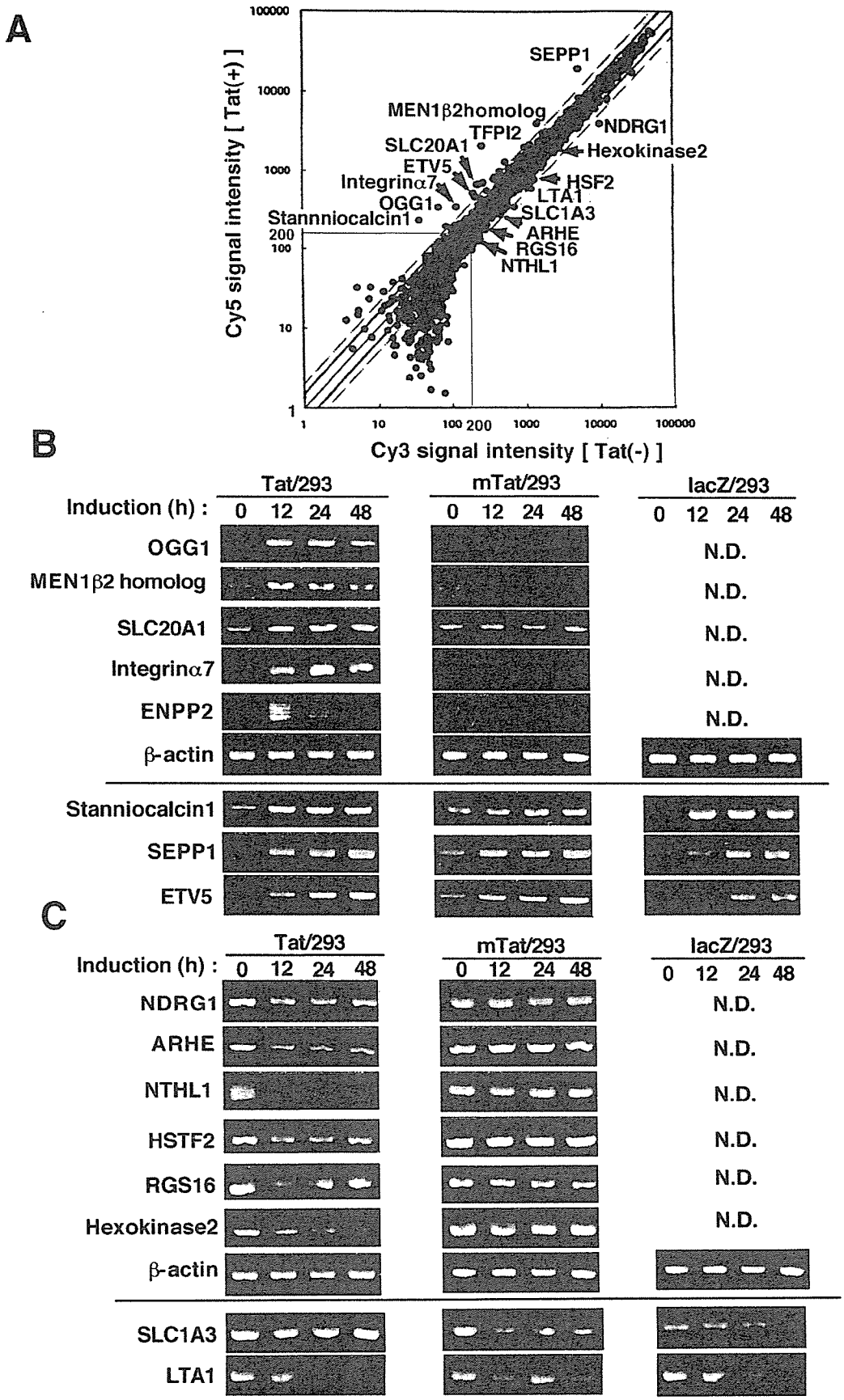

FIG. 2. **Gene expression profile analysis and confirmatory RT-PCR.** *A*, scatter plot of the hybridization signal intensity of genes in cells expressing Tat *versus* control cells. The mRNA was isolated from Tat/293 cells without (control) or with PonA treatment for 24 h. The cDNA probes were synthesized from the mRNA of each cell culture and labeled with either Cy5 (for Tat-expressing cells) or Cy3 (for control 293 cells). These probes were hybridized, in combination, to a gene chip (human 3K DNA CHIP™). The signal intensity of each gene on the microarray chip was

TABLE I
Genes up-regulated by Tat

Gene	Induction 12 h	Induction 24 h	GenBank™ accession no.
	-fold		
TFPI2[a]	6.5[b]	7.9 ± 0.7[c]	NM_006528
Stanniocalcin-1[a]	2.4	4.0 ± 0.3	NM_003155
SEPP1[a]	2.4	3.4 ± 0.3	NM_005410
OGG1	2.6	2.7 ± 0.2	NM_016819
Human clone 137308 mRNA; similar to *MEN1β*$_2$[d]	1.1	2.7 ± 0.2	U60873
ETV5 (Ets-related molecule)[a]	1.8	2.6 ± 0.2	NM_004454
Homo sapiens cDNA, similar to *MEN1β*$_2$[d]	1.1	2.5 ± 0.2	AK027191
SLC20A1	1.8	2.5 ± 0.3	NM_005415
Integrin α7	1.9	2.4 ± 0.1	NM_002206
ENPP2/autotaxin	1.7	2.3 ± 0.2	NM_006209
ABCG1 (ATP-binding cassette, subfamily G (WHITE), member 1)	1.3	2.1 ± 0.1	NM_004915
Calcium-binding protein p22	2.1	2.0 ± 0.1	BC001646
Laminin α3	1.4	2.0 ± 0.1	NM_000227

[a] Nonspecifically up-regulated by PonA treatment (see Fig. 2 for the results of RT-PCR).
[b] Data from single determinations 12 h after Tat induction.
[c] Data from triplicate determinations 24 h after Tat induction (expressed as means ± S.D.).
[d] Different cDNA segments of the same gene.

TABLE II
Genes down-regulated by Tat

Gene	Induction 12 h	Induction 24 h	GenBank™ accession no.
	-fold		
NDRG1	0.5[a]	0.4 ± 0.1[b]	NM_006096
ARHE	0.5	0.5 ± 0.1	NM_005168
SLC1A3[c]	0.7	0.5 ± 0.1	NM_004172
NTHL1	0.8	0.6 ± 0.1	NM_002528
HSTF2	0.5	0.6 ± 0.1	NM_004506
RGS16	0.7	0.6 ± 0.1	NM_002928
Hexokinase-2	0.7	0.6 ± 0.1	NM_000189
LTA1[c]	1.3	0.6 ± 0.2	AF104032

[a] Data from single determinations 12 h after Tat induction.
[b] Data from triplicate determinations 24 h after Tat induction (expressed as means ± S.D.).
[c] Nonspecifically up-regulated by PonA treatment (see Fig. 2 for the results of RT-PCR).

addition, H_2O_2 and oxidative stress inducers such as inflammatory cytokines (tumor necrosis factor-α and interleukin-1β) and lipopolysaccharide could not up-regulate *OGG1* gene expression (Fig. 4*D*, *right panel*). In support of these findings, when we performed transient luciferase assay using the *OGG1* promoter construct, no *OGG1* induction by these stimuli was observed (data not shown), consistent with a previous report by Dhénaut *et al.* (37). Therefore, it is unlikely that Tat induces *OGG1* expression through ROS production.

Transactivation of OGG1 by Tat—These observations prompted us to examine the possibility that Tat-mediated *OGG1* expression is the direct effect of Tat. We thus examined the effect of Tat on *OGG1* promoter activity. The transient luciferase assay was performed on various regions of the *OGG1* promoter linked to the luciferase reporter gene (Fig. 5). As shown in Fig. 5*A*, Tat stimulated the transcriptional activity of the reporter constructs containing the sequence upstream from position −472. Whereas the sequence upstream from position −945 was dispensable for Tat-mediated transactivation, no such effect was observed when the region spanning positions −945 to −472 was deleted (Fig. 5*A*, *lower left panel*). In 293 cells expressing mTat, no induction of *OGG1* promoter activity (other than the constitutive transcriptional activity) was observed. We also examined the Tat-mediated transactivation of the *OGG1* promoter in Jurkat cells and obtained essentially the same results (Fig. 5*A*, *lower right panel*).

Thus, Tat appears to transactivate *OGG1* expression through transcription factors located within the *OGG1* promoter region from positions −945 to −472. To further elucidate the mechanism by which Tat induces *OGG1* transcription, we created specific mutants lacking binding sites for GATA, AP-4, and/or AP-2 located in this region. When AP-4 sites were mutated, Tat no longer augmented the promoter activity (Fig. 5*B*, *black bars*). However, no reduction in Tat-mediated transactivation was observed when other sites were mutated. In addition, the basal promoter activity was augmented when the 5′-AP-4 site was mutated, whereas mutation of the GATA, AP-2, and 3′-AP-4 sites had little effect on the basal *OGG1* promoter activity (Fig. 5*B*, *hatched bars*), indicating that AP-4 acts as a transcriptional repressor of *OGG1* expression. These results suggest that AP-4 sites are required for Tat-induced *OGG1* gene expression and that the 5′-AP-4 site negatively regulates *OGG1* gene expression. In fact, overexpression of AP-4 inhibited both the Tat-stimulated and basal levels of *OGG1* gene expression without affecting the level of Tat expression (Fig. 5*C*).

Tat Interacts with AP-4 and Removes It from the OGG1 Promoter—To further investigate the mechanism by which Tat stimulates *OGG1* gene expression, we first examined the effect of Tat on AP-4 DNA binding by electrophoretic mobility shift assay. As shown in Fig. 6*A*, constitutive AP-4 DNA binding was observed in the cells, and a significant reduction in AP-4 DNA binding was observed when Tat was induced by PonA treatment. No such effect was observed when mTat was expressed. We then examined whether Tat associates with AP-4 in cultured cells by co-immunoprecipitation with either Tat (FLAG epitope-tagged) or AP-4 (Myc epitope-tagged). As shown in Fig. 6*B*, when Tat was immunoprecipitated with anti-FLAG antibody, endogenous AP-4 protein was detected within the immune complex. No AP-4 was co-immunoprecipitated with mTat. Conversely, when AP-4 was immunoprecipitated with

plotted. Genes with a signal intensity <200 U (of Cy5 and Cy3) were excluded from further analysis. *Solid* and *dashed lines* indicate the upper and lower boundaries of 1.5- and 2.0-fold changes, respectively. *B* and *C*, confirmation of genes up- or down-regulated by Tat using RT-PCR. *B*, genes up-regulated by Tat. Up-regulation of the stanniocalcin-1, *SEPP1*, and *ETV5* genes observed in cDNA array analysis appeared to be unspecific. *C*, genes down-regulated by Tat. Down-regulation of the *SLC1A3* and *LTA1* genes was considered nonspecific. RT-PCR analysis was performed with gene-specific primers and total RNA prepared from Tat/293, mTat/293, and LacZ/293 cells. Each cell culture was treated with PonA (10 μM) for the indicated periods of time. *N.D.*, not determined.

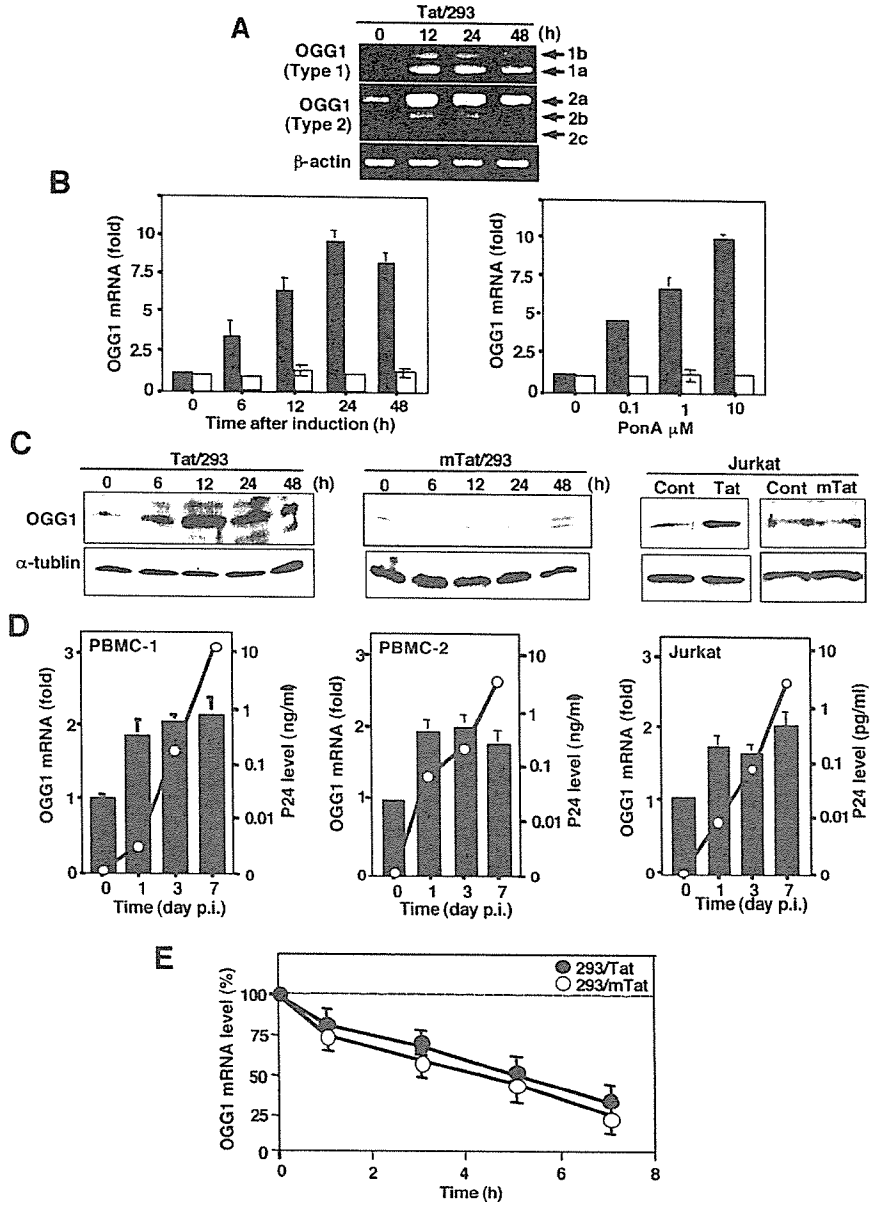

FIG. 3. **Induction of OGG1 by Tat.** *A*, induction of *OGG1* mRNA species by Tat. Tat/293 cells were treated with PonA (10 μM) for the indicated periods of time. RT-PCR analysis was performed with specific primers for the *OGG1* type 1 and 2 genes. Note that all of the splicing variants of *OGG1* mRNA were similarly up-regulated by Tat. *B*, quantitation of *OGG1* mRNA induction by real-time RT-PCR analysis. Tat/293 (*black bars*) and mTat/293 (*white bars*) cells were treated with 10 μM PonA for the indicated periods of time (*left panel*) or for 24 h with various concentrations of PonA (*right panel*). The total RNA was purified from each culture preparation and subjected to real-time RT-PCR using an *OGG1* primer/probe mixture. *C*, induction of OGG1 protein by Tat. Tat/293 (*left panel*) and mTat/293 (*middle panel*) cells were treated with PonA (10 μM) for the indicated periods of time, and OGG1 proteins were examined by Western blotting with anti-OGG1 antibody. Jurkat cells (*right panel*) were transfected with pcDNA-Tat, pcDNA-mTat, or the control (*Cont*) plasmid for 24 h. *D*, induction of *OGG1* mRNA by HIV-1 infection. PBMCs from two individuals and Jurkat cells were infected with HIV-1_{MN} at 100 $TCID_{50}$, and the *OGG1* RNA levels were measured by real-time RT-PCR. HIV-1 production was measured by the viral p24 antigen level in the culture supernatants. *p.i.*, post-infection in days. *E*, effect of Tat on *OGG1* mRNA stability. Tat/293 and mTat/293 cells were treated with PonA (10 μM) for 24 h and treated with actinomycin D (2 μg/ml). Total cellular RNA was obtained at the indicated time points, and the amount of *OGG1* mRNA was determined by real-time RT-PCR analysis. The experiments were performed in triplicate.

anti-Myc antibody, Tat (but not mTat) was co-immunoprecipitated (Fig. 6*B*, *lower panels*).

Furthermore, the ChIP assay was performed to examine whether the inhibition of AP-4 DNA binding by Tat occurs at the endogenous *OGG1* gene promoter. Tat/293 and mTat/293 cells were transfected with plasmids expressing Myc-tagged AP-4 or Myc-tagged LacZ (control), stimulated with PonA to express Tat or mTat, treated with formamide, and sonicated, and the cross-linked protein·DNA complex was immunoprecipitated with specific antibodies recognizing the Myc (AP-4) or V5 (Tat) epitope. The immunoprecipitated DNA was analyzed by PCR using primer pairs for the AP-4-binding sites within the *OGG1* promoter (−615 to −450). As demonstrated in Fig. 6*C*, a significant reduction in AP-4 bound to the *OGG1* promoter DNA was observed, and the extent of reduction was proportionate to the amount of Tat expressed (corresponding to the time-dependent expression of Tat in Fig. 1). No such effect was observed when mTat was expressed. The antibody to Tat precipitated the *OGG1* promoter (Fig. 6*C*, *left panels*), indicating that the Tat·AP-4·DNA ternary complex may be transiently formed. These observations indicate that Tat directly activates *OGG1* gene expression through sequestrating AP-4, a negative transcriptional regulator of *OGG1* expression.

Reduction of 8-Oxo-dG Levels by Tat and Effect of OGG1 Knockdown—Because OGG1 is responsible for the excision/repair of the oxidation-damaged DNA by excising 8-oxo-dG (30) and because Tat induces expression of OGG1, we measured the amounts of 8-oxo-dG in the cellular DNA by the HPLC-ECD method (26). Fig. 7*A* shows the levels of 8-oxo-dG before and after Tat expression. In control cells, the level of 8-oxo-dG was 8.7 ± 0.34 residues/10^6 dG residues (Fig. 7*B*). However, upon expression of Tat, the 8-oxo-dG levels were reduced to 7.7 ± 1.6 (0.89-fold), 5.6 ± 0.30 (0.64-fold), and 4.5 ± 1.2 (0.52-fold) residues/10^6 dG residues after 6, 12, and 24 h of Tat induction, respectively. Statistically significant reduction was observed after 12 and 24 h of Tat induction. No significant reduction in 8-oxo-dG levels was observed when mTat was expressed. Taken together, these observations indicate that Tat prevents accumulation of 8-oxo-dG by directly up-regulating OGG1 expression.

To confirm these findings, we adopted a siRNA technique to specifically knock down *OGG1* mRNA and examined the effect of Tat on the level of 8-oxo-dG when endogenous OGG1 was

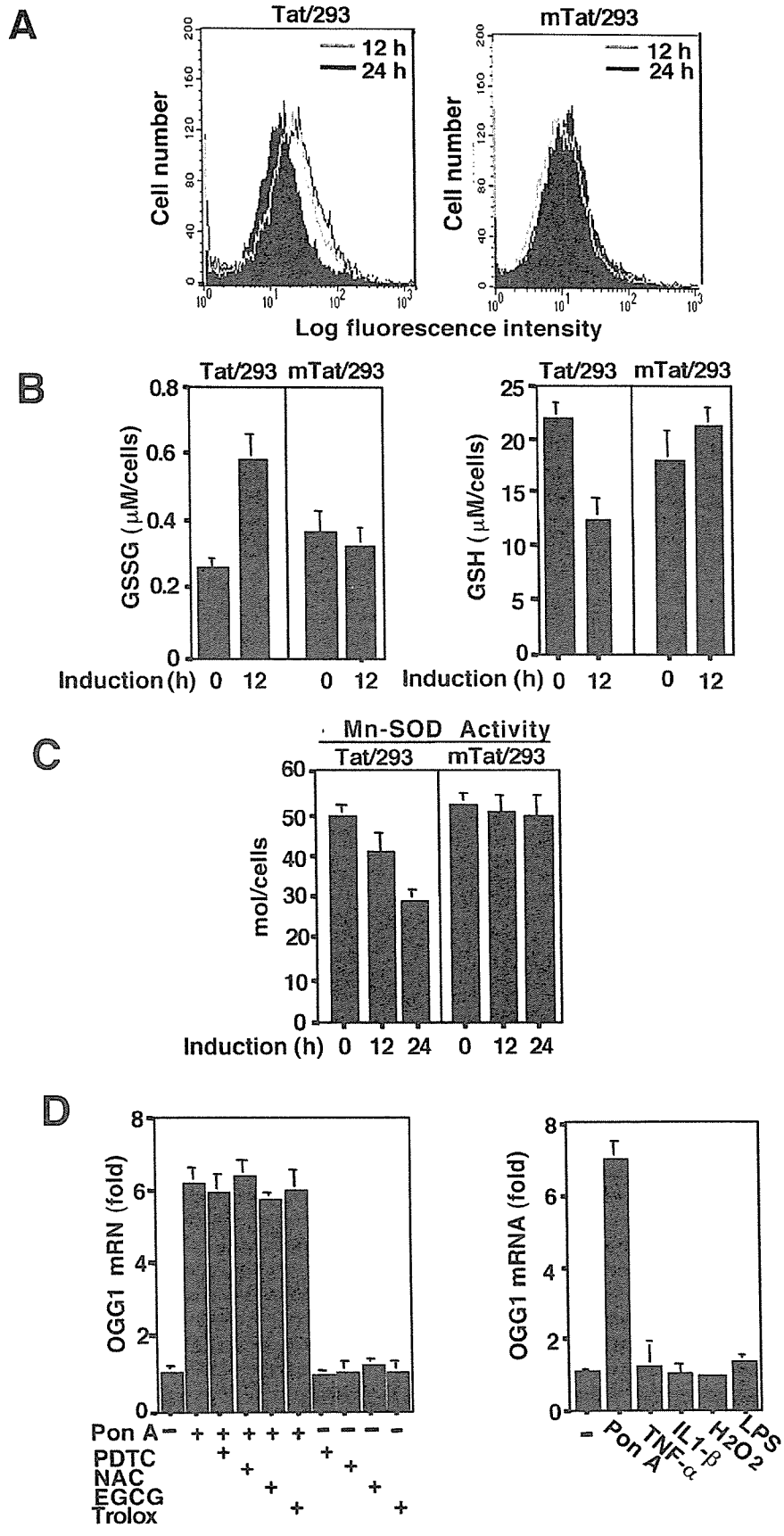

FIG. 4. **Induction of oxidative stress by Tat and effects of antioxidants on Tat-mediated *OGG1* expression.** *A*, accumulation of ROS by Tat. Tat/293 (*left panel*) and mTat/293 (*right panel*) cells were treated with 5 μM 2′,7′-dichlorofluorescein diacetate for 30 min, followed by treatment with PonA (10 μM) for 12 or 24 h. The intracellular 5,6-carboxy-2′,7′-dichlorofluorescein level (the indicator for ROS) in the cells was measured by flow cytometry. *B*, changes in GSSG (*left panel*) and GSH (*right panel*) contents by Tat. Tat/293 and mTat/293 cells were treated with PonA at 10 μM for 12 h, and GSH and GSSG contents were determined by the 5,5′-dithiobis(2-nitrobenzoic acid)/GSH reductase recycling method. To measure the GSSG content, GSH was masked by treatment with 2-vinylpyridine and triethanolamine prior to the reaction with GSH reductase and NADPH. *C*, inhibition of manganese superoxide dismutase (*Mn-SOD*) activity by Tat. Tat/293 and mTat/293 cells were treated with PonA (10 μM) for 12 or 24 h. The lysates were treated with KCN to mask copper superoxide dismutase and zinc superoxide dismutase activities, and then the manganese superoxide dismutase activity was measured by enzymatic assay. *D*, effects of various antioxidants on Tat-induced *OGG1* expression. Total RNA was prepared from each cell culture, and *OGG1* mRNA was quantitated by real-time RT-PCR as described in the legend to Fig. 2*B*. *Left panel*, Tat/293 cells were pretreated for 1 h with pyrrolidine dithiocarbamate (*PDTC*; 100 μM), *N*-acetyl-L-cysteine (*NAC*; 20 mM), epigallocatechin gallate (*EGCG*; 20 μM), or Trolox (100 μM) and stimulated with PonA (10 μM) for 12 h, and total RNA was prepared. *Right panel*, Tat/293 cells were treated with tumor necrosis factor-α (*TNF-α*; 5 ng/ml), interleukin-1β (*IL-1β*; 10 ng/ml), H_2O_2 (1 mM), lipopolysaccharide (*LPS*; 200 ng/ml), or PonA (10 μM) for 12 h, and the *OGG1* RNA levels were measured.

depleted. We synthesized three kinds of 21-nucleotide siRNA duplexes corresponding to the conserved *OGG1* mRNA regions utilized in all types of *OGG1* mRNA species. Cells transduced with OGG1 siRNA (No. 1) showed the greatest reduction in OGG1 protein levels compared with the control (Fig. 7*C*) and were thus used in the following experiment. As demonstrated

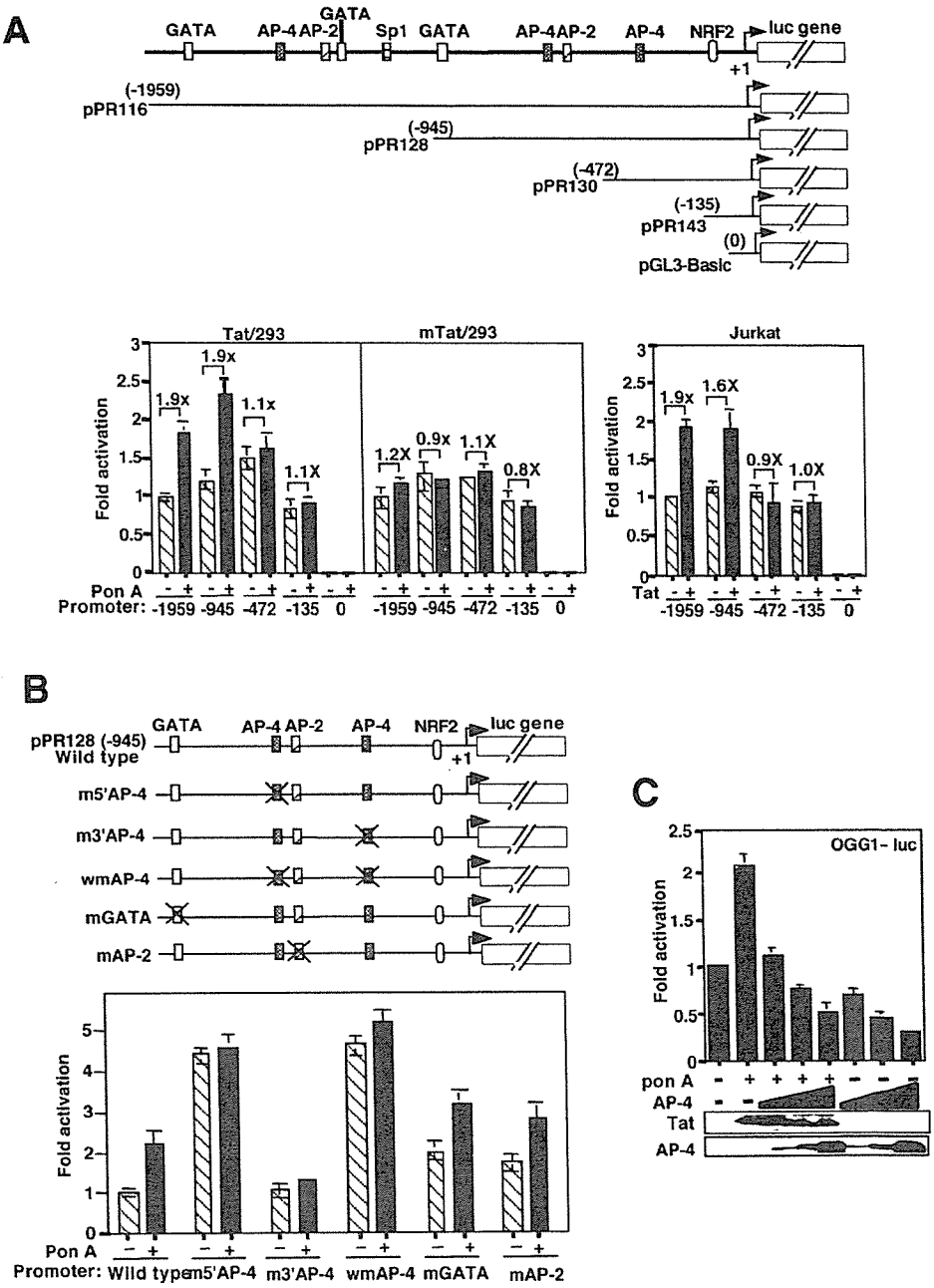

FIG. 5. **Tat directly activates *OGG1* gene expression.** *A*, effect of Tat on *OGG1* promoter activity. Schematic diagrams of the *OGG1* promoter constructs are shown, indicating the positions of various *cis*-elements for transcription factors GATA, AP-4, AP-2, Sp1, and NRF2 (nuclear factor erythroid-related factor 2) (*upper panel*). Tat/293 and mTat/293 cells (*lower left panel*) were transfected with various *OGG1* promoter constructs, incubated for 24 h, and treated (*black bars*) or not (*hatched bars*) with PonA (10 μM) for an additional 24 h. Jurkat cells (*lower right panel*) were transfected with *OGG1* promoter constructs in the presence (*black bars*) or absence (*hatched bars*) of pcDNA-Tat. Cells were harvested, and the luciferase (*luc*) activity was measured. The data are presented as the -fold increase in luciferase activity (means ± S.D.) relative to the transcriptional activity of the full-length *OGG1* promoter (pPR116) from three independent experiments. *B*, involvement of AP-4 in Tat-mediated *OGG1* expression. Various mutations in the binding sites for GATA, AP-4, and AP-2 were introduced into a wild-type *OGG1* promoter (pPR128-luc), and the effects of Tat were examined. Schematic representations of wild-type and mutant pPR128-luc constructs are shown (*upper panel*). Tat/293 cells were transfected with these reporter constructs, and the effects of Tat were similarly examined (*lower panel*). Note the increase in basal promoter levels with mutants containing a substitution in the 5′-AP-4 site and the lack of Tat response in mutants containing 5′- and/or 3′-AP-4 sites. *C*, repression of *OGG1* expression by AP-4. Tat/293 cells were transfected with pPR116-luc together with various amounts of plasmid expressing Myc-AP-4, incubated for 24 h, and treated with PonA (10 μM) for an additional 24 h to induce Tat expression (*upper panel*). The dose-dependent expression of AP-4 was revealed by Western blotting with anti-Myc tag antibody (*lower panels*). Tat protein expression was monitored using anti-FLAG antibody.

in Fig. 7*D*, OGG1 depletion by OGG1 siRNA (No. 1) resulted in a significant increase in the level of 8-oxo-dG (1.6-fold with the control and 1.4-fold with control siRNA). More important, 8-oxo-dG formation was induced by Tat when OGG1 was depleted (2.2-fold with the control and 1.9-fold with control siRNA). In addition, overexpression of AP-4, acting as a negative regulator of *OGG1* expression, increased the level of 8-oxo-dG (1.8-fold with the control).

DISCUSSION

In this study, we have explored the biological effects of Tat using gene expression profile analysis. We found that (i) Tat induces the *OGG1* gene and that (ii) Tat down-regulates the *NDRG1*, *RSG16*, and hexokinase-2 genes. The latter genes are known to be under the transcriptional control of p53 (46–48). Interestingly, Li *et al.* (49) observed the repression of p53 mRNA by Tat. Moreover, Tat was shown to directly inactivate p53 by protein-protein interaction (50, 52). Thus, the Tat-mediated down-regulation of these genes is consistent with previous findings. However, Tat-mediated OGG1 induction has not been reported. Thus, in this study, we analyzed the mechanism by which Tat induces *OGG1* gene expression.

We found that Tat-mediated OGG1 induction is not through stabilization of the *OGG1* mRNA. In addition, Tat-mediated *OGG1* induction was not reversed by treatment with antioxidants, indicating that Tat-mediated *OGG1* induction could not be attributable to oxidative stress induced by Tat. By performing transient luciferase assay using the reporter plasmid containing various regions of *OGG1*, we found that Tat induces *OGG1* gene expression through the central AP-4 site (located at positions −545 to −540) in its upstream region. Although AP-4 is known to activate expression of the SV40 (53) and transforming growth factor-β (54) genes, it is also known to repress expression of the human angiotensinogen (55) and HIV-1 (56) genes, although the mechanism of AP-4 action has not been clarified. Our experiments have revealed that AP-4 negatively regulates *OGG1* gene expression via binding to the central

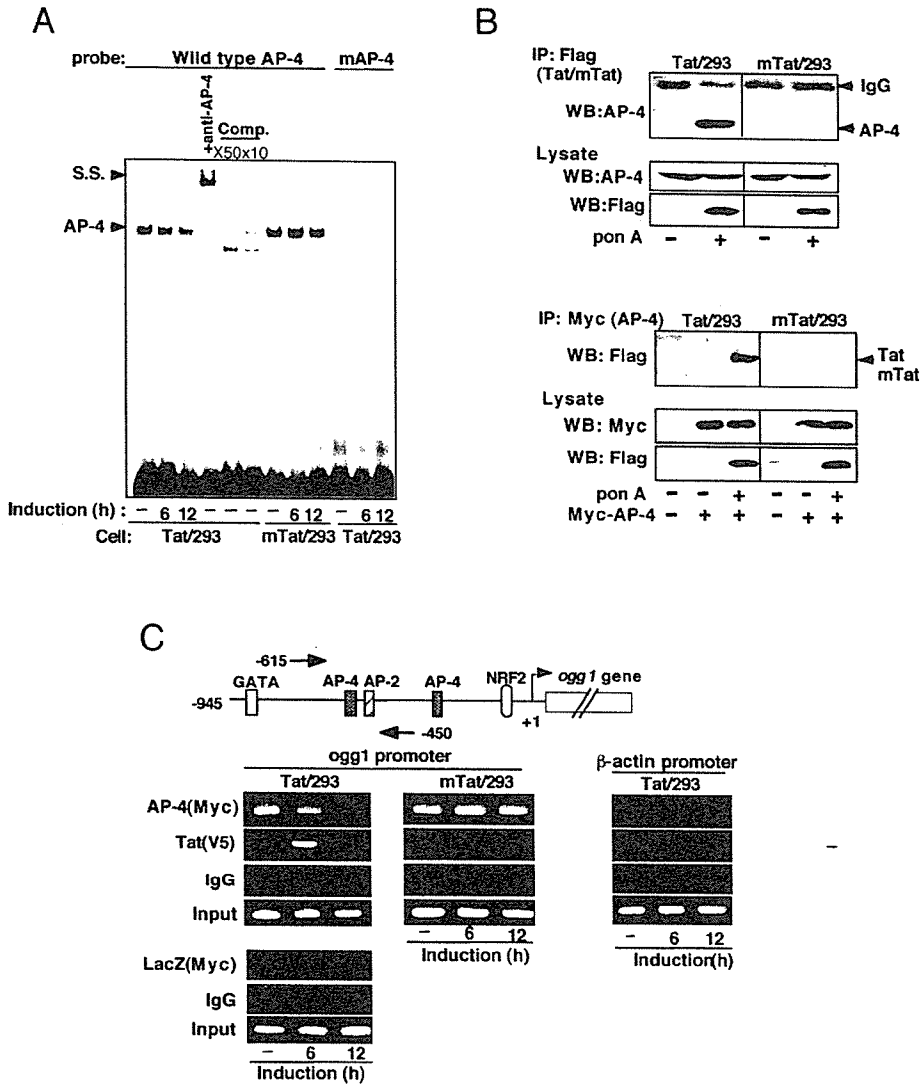

FIG. 6. **Mechanism by which Tat induces *OGG1* gene expression: Tat interacts with AP-4 and removes AP-4 from the *OGG1* promoter.** *A*, effect of Tat on AP-4 DNA binding. Nuclear extracts were prepared from Tat/293 and mTat/293 cells, and AP-4 DNA binding was examined by electrophoretic mobility shift assay using AP-4 or mutant AP-4 probes. To verify the AP-4·DNA complex, nuclear extracts were incubated with anti-AP-4 antibody or excess amounts of competitor oligonucleotides (10- or 50-fold). The positions of the specific protein·DNA and supershifted (*S.S.*) complexes (*arrowheads*) are indicated. *B*, interaction between Tat and AP-4 *in vivo*. *Upper panel*, cell lysates were prepared, and immune complexes containing Tat or mTat were immunoprecipitated (*IP*) with anti-FLAG antibody (detecting Tat). The immunoprecipitates were separated by SDS-PAGE, followed by Western blotting (*WB*) with anti-AP-4 antibody. One-tenth of each protein lysate used in each reaction was loaded as the input control. *Lower panels*, Tat/293 and mTat/293 cells were transfected with plasmid expressing Myc-AP-4, and expression of Tat proteins was induced by PonA (10 μM). The cell lysates were immunoprecipitated with anti-Myc antibody (detecting AP-4), and the immune complex was analyzed for the presence of Tat by Western blotting with anti-FLAG antibody. *C*, ChIP assay. *Upper panel*, the *OGG1* promoter region amplified by the primer pairs in ChIP assay is illustrated. *Arrows* indicate the positions of PCR primers. *Lower panels*, cell lysates were prepared from Tat/293 and mTat/293 cells that were transfected with plasmid expressing Myc-AP-4 or Myc-LacZ (control) and treated with PonA (10 μM) for expression of Tat and mTat. Cross-linked chromatin fragments were prepared, and the association of AP-4, LacZ, Tat, and *OGG1* promoter DNA was analyzed by ChIP assay. The recovered DNA was amplified by PCR with promoter-specific primers and analyzed on a 2% agarose gel. DNAs isolated from sonicated cross-linked chromatin fragments were used as inputs. The β-actin promoter DNA was similarly analyzed as a control.

AP-4 site and that Tat activates *OGG1* promoter activity by sequestrating AP-4 from the *OGG1* promoter. Thus, the positive effect of Tat on *OGG1* gene expression appears to be a direct effect.

Intriguingly, we observed that the extent of oxidation-induced guanosine modification (8-oxo-dG) was reduced, although Tat induced oxidative stress as revealed by the increase in ROS and GSSG and the decrease in manganese superoxide dismutase activity. When OGG1 expression was knocked down by siRNA, the amount of 8-oxo-dG was increased, suggesting that the Tat-induced reduction of 8-oxo-dG requires *OGG1* gene expression and that the Tat-mediated induction of OGG1 appears to be independent of Tat pro-oxidant action.

Thus, in addition to its crucial role in viral replication, Tat appears to play a role in maintenance of the genetic integrity of proviral and host cell DNAs. Although various conditions associated with HIV infection and replication are pro-oxidant (12, 13, 57–59), the observed mutations accumulated within the HIV genome have been revealed to be in favor of the G:C to A:T transition (18–22) rather than the G:C to T:A transversion mediated by the oxidative modification. This is in contrast with most of the mutations associated with human cancers, where the G:C to T:A transversion is predominant (28, 29). If induction of OGG1 were through oxidative stress associated with Tat actions, the level of 8-oxo-dG should have been higher in Tat-expressing cells than in control cells. These findings indicate that Tat-mediated OGG1 induction is more than a feedback action. Although additional studies are needed, such as the

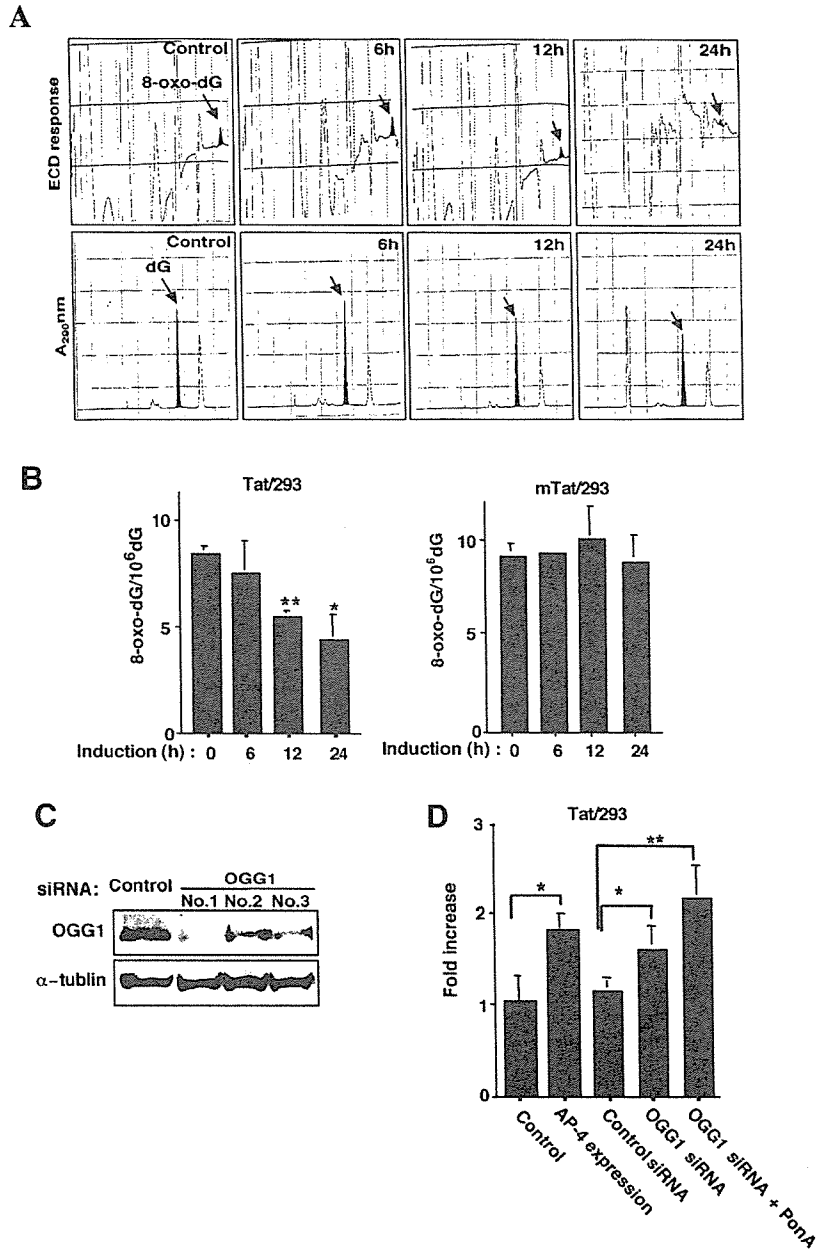

FIG. 7. **Reduction in the levels of 8-oxo-dG by Tat.** *A*, electrochemical chromatographs of 8-oxo-dG. The HPLC patterns were traced using an ECD. The 8-oxo-dG peaks (ECD response; *shaded areas* in the *upper panels*) are indicated by *arrows*. The dG peaks (absorption at 290 nm; *shaded areas* in the *lower panels*) are also indicated. Cells were treated for the indicated periods of time with PonA (10 μM) to express Tat or mTat. Nuclear DNA samples were prepared and measured for 8-oxo-dG levels. DNA was digested to obtain deoxynucleosides and analyzed with an HPLC-ECD system as described under "Experimental Procedures." *B*, levels of 8-oxo-dG in DNA expressing Tat or mTat. The amount of 8-oxo-dG is expressed as the number of 8-oxo-dG residues/10^6 dG residues. The results represent the means ± S.D. from four independent experiments. *, $p < 0.005$; **, $p < 0.001$. *C*, OGG1 knockdown by siRNA. Tat/293 cells were transfected with 100 nM siRNAs directed against various portions of OGG1 (Nos. 1–3) or green fluorescent protein (control) mRNAs. After 72 h of transfection, cells were lysed, and OGG1 protein levels were assessed by Western blotting with anti-OGG1 antibody (*upper panel*). The blot was stripped and reprobed with anti-α-tubulin antibody (*lower panel*). *D*, effects of OGG1 depletion and expression of Tat and AP-4 on the levels of 8-oxo-dG. *First bar*, control Tat/293 cells (no treatment); *second bar*, Tat/293 cells transfected with plasmid expressing AP-4; *third* and *fourth bars*, Tat/293 cells transfected with siRNA against green fluorescent protein (siRNA control) or OGG1 (No. 1), respectively, and incubated for 72 h; *fifth bar*, Tat/293 cells transfected with siRNA against OGG1 (No. 1) for 48 h and treated with PonA to induce Tat expression for an additional 24 h. At 72 h post-transfection, nuclear DNA samples were extracted, and the levels of 8-oxo-dG were measured similarly as described for *A*. The levels of 8-oxo-dG are shown as the -fold increase compared with the level of the no-treatment sample (*first bar*). *, $p < 0.05$; **, $p < 0.01$.

effect of OGG1 mutation on the extent of mutation of viral and cellular genomes during chronic HIV infection, the Tat-mediated induction of OGG1 could be viewed as a regulated "feed-forward" mechanism.

Acknowledgments—We thank Drs. J. P. Radicella and L. Naumovski for providing the plasmid constructs containing various portions of the *OGG1* promoter and 293/LacZ cells, respectively. We also thank A. Victoriano for language revision.

REFERENCES

1. Jones, K. A., and Peterlin, B. M. (1994) *Annu. Rev. Biochem.* **63,** 717–743
2. Berkhout, B., Silverman, R. H., and Jeang, K. T. (1989) *Cell* **59,** 273–282
3. Okamoto, T., and Wong-Staal, F. (1986) *Cell* 29–35
4. Okamoto, H., Sheline, C. T., Corden, J. L., Jones, K. A., and Peterlin, B. M. (1996) *Proc. Natl. Acad. Sci. U. S. A.* **93,** 11575–11579
5. Wei, P., Garber, M. E., Fang, S. M., Fischer, W. H., and Jones, K. A. (1998) *Cell* **92,** 451–462
6. Kanazawa, S., Okamoto, T., and Peterlin, B. M. (2000) *Immunity* **12,** 61–70
7. Mancebo, H. S., Lee, G., Flygare, J., Tomassini, J., Luu, P., Zhu, Y., Peng, J., Blau, C., Hazuda, D., Price, D., and Flores, O. (1997) *Genes Dev.* **11,** 2633–2644
8. Zhu, Y., Pe'ery, T., Peng, J., Ramanathan, Y., Marshall, N., Marshall, T., Amendt, B., Mathews, M. B., and Price, D. H. (1997) *Genes Dev.* **11,** 2622–2632
9. Marzio, G., Tyagi, M., Gutierrez, M. I., and Giacca, M. (1998) *Proc. Natl. Acad. Sci. U. S. A.* **95,** 13519–13524
10. Price, D. H. (2000) *Mol. Cell. Biol.* **20,** 2629–2634
11. Zauli, G., Gibellini, D., Milani, D., Mazzoni, M., Borgatti, P., La Placa, M., and Capitani, S. (1993) *Cancer Res.* **53,** 4481–4485
12. Flores, S. C., Marecki, J. C., Harper, K. P., Bose, S. K., Nelson, S. K., and McCord, J. M. (1993) *Proc. Natl. Acad. Sci. U. S. A.* **90,** 7632–7636
13. Westendorp, M. O., Shatrov, V. A., Schulze-Osthoff, K., Frank, R., Kraft, M., Los, M., Krammer, P. H., Droge, W., and Lehmann, V. (1995) *EMBO J.* **14,** 546–554
14. Conant, K., Garzino-Demo, A., Nath, A., McArthur, J. C., Halliday, W., Power, C., Gallo, R. C., and Major, E. O. (1998) *Proc. Natl. Acad. Sci. U. S. A.* **95,** 3117–3121
15. Izmailova, E., Bertley, F. M., Huang, Q., Makori, N., Miller, C. J., Young, R. A., and Aldovini, A. (2003) *Nat. Med.* **9,** 191–197
16. Choi, J., Liu, R. M., Kundu, R. K., Sangiorgi, F., Wu, W., Maxson, R., and Forman, H. J. (2000) *J. Biol. Chem.* **275,** 3693–3698
17. Kumar, A., Manna, S. K., Dhawan, S., and Aggarwal, B. B. (1998) *J. Immunol.* **161,** 776–781
18. Li, Y., Kappes, J. C., Conway, J. A., Price, R. W., Shaw, G. M., and Hahn, B. H. (1991) *J. Virol.* **65,** 3973–3985
19. Moriyama, E. N., Ina, Y., Ikeo, K., Shimizu, N., and Gojobori, T. (1991) *J. Mol. Evol.* **32,** 360–363
20. Perry, S. T., Flaherty, M. T., Kelley, M. J., Clabough, D. L., Tronick, S. R., Coggins, L., Whetter, L., Lengel, C. R., and Fuller, F. (1992) *J. Virol.* **66,** 4085–4097
21. Vartanian, J. P., Meyerhans, A., Asjo, A., and Wain-Hobson, S. (1991) *J. Virol.* **65,** 1779–1788
22. Harris, R. S., Bishop, K. N., Sheehy, A. M., Craig, H. M., Petersen-Mahrt,

S. K., Watt, I. N., Neuberger, M. S., and Malim, M. H. (2003) *Cell* **113,** 803–809
23. Mangeat, B., Turelli, P., Caron, G., Friedli, M., Perrin, L., and Trono, D. (2003) *Nature* **424,** 99–103
24. Mariani, R., Chen, D., Schrofelbauer, B., Navarro, F., Konig, R., Bollman, B., Munk, C., Nymark-McMahon, H., and Landau, N. R. (2003) *Cell* **114,** 21–31
25. Zhang, H., Yang, B., Pomerantz, R. J., Zhang, C., Arunachalam, S. C., and Gao, L. (2003) *Nature* **424,** 94–98
26. Kasai, H., and Nishimura, S. (1984) *Nucleic Acids Res.* **12,** 2137–2145
27. Kasai, H. (1997) *Mutat. Res.* **387,** 147–163
28. Hatahet, Z., Zhou, M., Reha-Krantz, L. J., Morrical, S. W., and Wallace, S. S. (1998) *Proc. Natl. Acad. Sci. U. S. A.* **95,** 8556–8561
29. Hussain, S. P., and Harris, C. C. (1998) *Cancer Res.* **58,** 4023–4037
30. Boiteux, S., and Radicella, J. P. (2000) *Arch. Biochem. Biophys.* **377,** 1–8
31. Radicella, J. P., Dherin, C., Desmaze, C., Fox, M. S., and Boiteux, S. (1997) *Proc. Natl. Acad. Sci. U. S. A.* **94,** 8010–8015
32. Rosenquist, T. A., Zharkov, D. O., and Grollman, A. P. (1997) *Proc. Natl. Acad. Sci. U. S. A.* **94,** 7429–7434
33. Arai, T., Kelly, V. P., Komoro, K., Minowa, O., Noda, T., and Nishimura, S. (2003) *Cancer Res.* **63,** 4287–4292
34. Minowa, O., Arai, T., Hirano, M., Monden, Y., Nakai, S., Fukuda, M., Itoh, M., Takano, H., Hippou, Y., Aburatani, H., Masumura, K., Nohmi, T., Nishimura, S., and Noda, T. (2000) *Proc. Natl. Acad. Sci. U. S. A.* **97,** 4156–4161
35. Okamoto, H., Cujec, T. P., Okamoto, M., Peterlin, B. M., Baba, M., and Okamoto, T. (2000) *Virology* **272,** 402–408
36. Takada, N., Sanda, T., Okamoto, H., Yang, J. P., Asamitsu, K., Sarol, L., Kimura, G., Uranishi, H., Tetsuka, T., and Okamoto, T. (2002) *J. Virol.* **76,** 8019–8030
37. Dhénaut, A., Boiteux, S., and Radicella, J. P. (2000) *Mutat. Res.* **461,** 109–118
38. Ao, Y., Rohde, L. H., and Naumovski, L. (2001) *Oncogene* **20,** 2720–2725
39. Ando, K., Kanazawa, S., Tetsuka, T., Ohta, S., Jiang, X., Tada, T., Kobayashi, M., Matsui, N., and Okamoto, T. (2003) *Oncogene* **22,** 7796–7803
40. Watanabe, N., Ando, K., Yoshida, S., Inuzuka, S., Kobayashi, M., Matsui, N., and Okamoto, T. (2002) *Biochem. Biophys. Res. Commun.* **294,** 1121–1129
41. Tetsuka, T., Uranishi, H., Imai, H., Ono, T., Sonta, S., Takahashi, N., Asamitsu, K., and Okamoto, T. (2000) *J. Biol. Chem.* **275,** 4383–4390
42. Sarol, L. C., Imai, K., Asamitsu, K., Tetsuka, T., Barzaga, N. G., and Okamoto, T. (2002) *Biochem. Biophys. Res. Commun.* **291,** 890–896
43. Pincus, S. H., Messer, K. G., and Hu, S. H. (1994) *J. Clin. Investig.* **93,** 140–146
44. Tsurudome, Y., Hirano, T., Yamato, H., Tanaka, I., Sagai, M., Hirano, H., Nagata, N., Itoh, H., and Kasai, H. (1999) *Carcinogenesis* **20,** 1573–1576
45. Saez, E., Nelson, M. C., Eshelman, B., Banayo, E., Koder, A., Cho, G. J., and Evans, R. M. (2000) *Proc. Natl. Acad. Sci. U. S. A.* **97,** 14512–14517
46. Buckbinder, L., Velasco-Miguel, S., Chen, Y., Xu, N., Talbott, R., Gelbert, L., Gao, J., Seizinger, B. R., Gutkind, J. S., and Kley, N. (1997) *Proc. Natl. Acad. Sci. U. S. A.* **94,** 7868–7872
47. Kurdistani, S. K., Arizti, P., Reimer, C. L., Sugrue, M. M., Aaronson, S. A., and Lee, S. W. (1998) *Cancer Res.* **58,** 4439–4444
48. Mathupala, S. P., Heese, C., and Pedersen, P. L. (1997) *J. Biol. Chem.* **272,** 22776–22780
49. Li, C. J., Wang, C., Friedman, D. J., and Pardee, A. B. (1995) *Proc. Natl. Acad. Sci. U. S. A.* **92,** 5461–5464
50. Longo, F., Marchetti, M. A., Castagnoli, L., Battaglia, P. A., and Gigliani, F. (1995) *Biochem. Biophys. Res. Commun.* **206,** 326–334
51. Nishioka, K., Ohtsubo, T., Oda, H., Fujiwara, T., Kang, D., Sugimachi, K., and Nakabeppu, Y. (1999) *Mol. Biol. Cell.* **10,** 1637–1652
52. Clark, E., Santiago, F., Deng, L., Chong, S., de La Fuente, C., Wang, L., Fu, P., Stein, D., Denny, T., Lanka, V., Mozafari, F., Okamoto, T., and Kashanchi, F. (2000) *J. Virol.* **74,** 5040–5052
53. Mermod, N., Williams, T. J., and Tjian, R. (1988) *Nature* **332,** 557–561
54. Andriamanalijaona, R., Felisaz, N., Kim, S. J., King-Jones, K., Lehmann, M., Pujol, J. P., and Boumediene, K. (2003) *Arthritis Rheum.* **48,** 1569–1581
55. Cui, Y., Narayanan, C. S., Zhou, J., and Kumar, A. (1998) *Gene (Amst.)* **224,** 97–107
56. Ou, S. H., Garcia-Martinez, L. F., Paulssen, E. J., and Gaynor, R. B. (1994) *J. Virol.* **68,** 7188–7199
57. Staal, F. J., Ela, S. W., Roederer, M., Anderson, M. T., Herzenberg, L. A., and Herzenberg, L. A. (1992) *Lancet* **339,** 909–912
58. Roederer, M., Staal, F. J., Raju, P. A., Ela, S. W., Herzenberg, L. A., and Herzenberg, L. A. (1990) *Proc. Natl. Acad. Sci. U. S. A.* **87,** 4884–4888
59. Kalebic, T., Kinter, A., Poli, G., Anderson, M. E., Meister, A., and Fauci, A. S. (1991) *Proc. Natl. Acad. Sci. U. S. A.* **88,** 986–990

THE JOURNAL OF BIOLOGICAL CHEMISTRY

Vol. 279, No. 30, Issue of July 23, pp. 31964–31972, 2004
Printed in U.S.A.

Human Immunodeficiency Virus Type 1 Gag Assembly through Assembly Intermediates*

Received for publication, December 9, 2003, and in revised form, April 27, 2004
Published, JBC Papers in Press, May 19, 2004, DOI 10.1074/jbc.M313432200

Yuko Morikawa‡§, Toshiyuki Goto¶, and Fumitaka Momose‡

From the ‡Kitasato Institute of Life Sciences, Kitasato University, Shirokane 5-9-1, Minato-ku, Tokyo 108-8641 and the ¶College of Medical Technology, Kyoto University, Kawahara-cho 53, Shogoin, Sakyo-ku, Kyoto 606-8507, Japan

Human immunodeficiency virus Gag protein self-assembles into spherical particles, and recent reports suggest the formation of assembly intermediates during the process. To understand the nature of such assembly intermediates along with the mechanism of Gag assembly, we employed expression in *Escherichia coli* and an *in vitro* assembly reaction. When *E. coli* expression was performed at 37 °C, Gag predominantly assembled to a high order of multimer, apparently equivalent to the virus-like particles obtained following Gag expression in eukaryotic cells, through the formation of low orders of multimer characterized with a discreet sedimentation value of 60 S. Electron microscopy confirmed the presence of spherical particles in the *E. coli* cells. In contrast, expression at 30 °C resulted in the production of only the 60 S form of Gag multimer, and crescent-shaped structures or small patches with double electron-dense layers were accumulated, but no complete particles. *In vitro* assembly reactions using purified Gag protein, when performed at 37 °C, also produced the high order of Gag multimers with some 60 S multimers, whereas the 30 °C reaction produced only the 60 S multimers. However, when the 60 S multimers were cross-linked so as not to allow conformational changes, *in vitro* assembly reactions at 37 °C did not produce any higher order of multimers. ATP depletion did not halt Gag assembly in the *E. coli* cells, and the addition of GroEL-GroES to *in vitro* reactions did not facilitate Gag assembly, indicating that conformational changes rather than protein refolding by chaperonins, induced at 37 °C, were solely responsible for the Gag assembly observed here. We suggest that Gag assembles to a capsid through the formation of the 60 S multimer, possibly a key intermediate of the assembly process, accompanied with conformational changes in Gag.

The major structural component of human immunodeficiency virus (HIV),[1] Gag, is the sole protein required for viral particle budding, and expression of Gag protein alone in eukaryotic cells produces Gag virus-like particle (VLP), morphologically identical to the immature form of HIV particles (1–3). The process of Gag assembly is thought to consist of N-terminal myristoylation of Gag followed by relocation to the plasma membrane and multimerization of Gag to form VLP. Three discrete Gag regions responsible for virus particle production have been identified by genetic studies and termed the membrane-binding, the interacting, and the late domains. The membrane-binding domain is located at the N-terminal matrix/membrane (MA) of Gag and contains a bipartite membrane-binding signal (N-terminal myristoylation and a cluster of basic amino acids) that directs the association of Gag with membrane (1, 4, 5). The interacting domain is essential for Gag-Gag interactions and spans from the central capsid (CA) to nucleocapsid (NC) of Gag (6–9). The late domain, responsible for pinching off viral particles from the membrane, has been found in the C-terminal p6 domain of Gag (10, 11) but, in high level of expression systems, is often dispensable (1, 2).

An HIV particle is composed of ~2000 Gag molecules (12) that are arranged in a high order form. In fact, studies by high resolution electron microscopy have revealed that Gag molecules are arranged in a fullerene- or cage-like network consisting of hexagonal and trigonal units (13, 14), suggesting the ordered multimerization of Gag in a virus particle. However, little is known about the mechanisms involved in the formation of Gag capsid. The process of building Gag up into capsid remains to be elucidated and includes such questions as whether assembly consists of multiple sets of reactions involving discrete intermediates or a single sequential reaction and, in both cases, what the mechanism of Gag multimerization might be.

A number of electron microscopy studies to date have provided evidence for electron-dense Gag layers underneath the plasma membrane and nascent particles connected to the cell surface by a thin stalk (15), suggesting that Gag assembles following membrane targeting and also suggesting that assembly intermediates, if any, would be similarly present on the membrane. Consistent with these observations, membrane-bound Gag complexes have been resolved on Optiprep density gradients (16). However, recent observations of Gag-expressing cells have revealed the occurrence of Gag complexes in the cytoplasm, suggesting Gag multimer formation prior to membrane relocation (17, 18). Similarly, data based on the detergent sensitivity of Gag complexes have suggested a detergent-resistant complex in the cytosol (19, 20), although these cytosolic Gag complexes may possibly be a dead end product (16, 21). These apparently conflicting results argue that the morphogenetic pathway of Gag assembly is not as clear cut as is commonly thought, but the data clearly show that some level of Gag multimer, plausibly assembly intermediates, occur during particle assembly. The definition of such intermediates would lead to a better understanding of the sequential nature of the Gag assembly reactions.

As a result of the lack of host *N*-myristoyltransferase, Gag expression in *Escherichia coli* confers neither *N*-myristoylation

* This work was supported by a Health Sciences Research Grant from the Ministry of Health, Labor and Welfare of Japan. The costs of publication of this article were defrayed in part by the payment of page charges. This article must therefore be hereby marked "*advertisement*" in accordance with 18 U.S.C. Section 1734 solely to indicate this fact.

§ To whom correspondence should be addressed. Tel.: 81-3-5791-6129; Fax: 81-3-5791-6268; E-mail morikawa@lisci.kitasato-u.ac.jp.

[1] The abbreviations used are: HIV, human immunodeficiency virus; VLP, virus-like particle; MA, matrix/membrane; CA, capsid; NC, nucleocapsid; DTBP, dimethyl 3,3′-dithiobispropionimidate; IPTG, isopropyl-β-D-thiogalactopyranoside; DSP, dithiobis.

(22) nor subsequent membrane relocation on the molecule but yields spherical particles inside the *E. coli* cells (23). The particles are a hollow sphere surrounded by an electron-dense ring structure, similar to the immature form of HIV VLPs produced by Gag expression in eukaryotic cells (24). Interestingly, spherical particles with similar morphologies are also produced when purified soluble Gag protein is subjected to *in vitro* assembly reactions (25, 26), although the particle sizes are heterogeneous when compared with those of VLPs produced by eukaryotic cells. Similar findings have been reported for other retroviral Gags (27, 28). These data show that the assembly phenotypes of Gag produced by expression in *E. coli* as well as by *in vitro* reaction mimic the authentic Gag assembly observed in eukaryotic cells and suggest that the assembly reaction is driven by the intrinsic properties of Gag protein. Similar conclusions were made when experiments were carried out with Gag fragments (*e.g.* MA-CA, CA, and CA-NC). For example, CA and CA-NC formed tubular or conical structures by *in vitro* assembly, and *E. coli* expression of these fragments yielded tubular structures in the cells, both of which may represent conical cores of mature HIV particles observed following Gag processing (24, 29, 30).

We have shown previously, using purified Gag protein lacking the C-terminal p6 domain, that the *in vitro* assembly reaction is composed of two sequential steps: the formation of a 60 S complex, possibly an assembly intermediate, and complete assembly to 600 S, equivalent to the immature form of HIV capsids (26). Although the ideal for study of Gag assembly would be in higher eukaryotic cell expression systems, the level of Gag expression in such systems is often insufficient for biochemical and structural analyses, and neither expression nor assembly of Gag is synchronized. To examine the nature of assembly intermediates along with the mechanism of assembly, we have employed an inducible expression system of *E. coli* and *in vitro* assembly reaction. Our data show that the 60 S forms of Gag multimers have a defined structure and detergent sensitivity, suggesting that they may be genuine Gag assembly intermediates. The data also suggest that the Gag assembly process may be accompanied by conformational changes in Gag.

EXPERIMENTAL PROCEDURES

Materials—*E. coli* expression vector pTrcHisA was purchased from Invitrogen, and metal chelate resin (HisBind Resin) was from Novagen. Sephadex G-25 (PD-10) and a high molecular weight calibration kit were purchased from Amersham Biosciences. Eukaryotic 80 S ribosome was kindly supplied by Kiyohisa Mizumoto (Kitasato University, Japan), and the immature forms of HIV Gag VLPs were purified from culture medium of *Spodoptera frugiperda* (*Sf*9) cells infected with a recombinant baculovirus containing the HIV-1 *gag* gene (31). Anti-HIV-1 CA mouse monoclonal antibody was obtained from Advanced Biotechnologies. Dithiobis (DSP) and dimethyl 3,3′-dithiobispropionimidate (DTBP) were purchased from Pierce Biotechnology, and GroEL-GroES mixture was from TaKaRa Shuzo Co. Ltd. Other reagents were commercially available of analytical grade.

DNA Construction and Protein Expression—The HIV-1 *gag* gene encoding the Gag region essential for virus particle formation (MA-CA-p2-NC) with the additional 6 histidine residues at the C terminus was cloned into *E. coli* expression vector pTrcHisA, as described previously (26). Transformed *E. coli* cells were cultured at 37 and 30 °C. Protein expression was carried out by the addition of isopropyl-β-D-thiogalactopyranoside (IPTG) at the log phase of *E. coli* growth. For ATP depletion, NaN_3 was added to the culture medium following IPTG induction, a method that was described previously (32, 33).

Preparation of Whole Cell Lysates and Protein Purification—For preparation of whole cell lysates, *E. coli* cells were harvested by centrifugation at 4 °C at 8,000 × *g* for 15 min and suspended in 50 mM Tris (pH 8.0), 150 mM NaCl, 5 mM EDTA, and 1 mM dithiothreitol. Following sonication at 4 °C for 15 min, the cells were lysed by the addition of 0.1% Nonidet P-40 and incubated at room temperature for 10 min in the presence of 10 μg/ml RNaseA. For protein purification, *E. coli* cells were suspended in binding buffer (20 mM Tris (pH 7.9), 150 mM NaCl, and 10 mM imidazole). Disruption by sonication, the addition of Nonidet P-40, and RNaseA treatment were carried out as before. The cell lysates were clarified by centrifugation at 15,000 × *g* for 30 min at 4 °C, and the supernatants were subjected to metal chelate chromatography (Novagen). Following extensive wash with binding buffer and subsequently with wash buffer (20 mM Tris (pH 7.9), 150 mM NaCl, and 60 mM imidazole), bound protein was eluted with elute buffer (20 mM Tris (pH 7.9), 150 mM NaCl, and 1 M imidazole). The details of the purification protocol have been described previously (26).

In Vitro Assembly Reaction—*In vitro* assembly reaction of purified Gag protein was performed as described previously (26). In brief, following metal chelate chromatography, eluted fractions were desalted using Sephadex G-25 (PD-10) equilibrated with buffer A (20 mM Tris (pH 8.6 adjusted at room temperature), 100 mM NaCl, 0.2 mM EDTA, 5 mM $MgCl_2$, and 1 mM dithiothreitol). For *in vitro* assembly, the desalted fractions were incubated at either 37 or 30 °C for 3 h. In some experiments, assembly intermediates of Gag were incubated in the presence of 10% (v/v) glycerol (see the legend for Fig. 8) or incubated with GroEL-GroES (with a Gag-to-GroEL-GroES molar ratio of 1:1) in the presence of 1 mM ATP or ATP-γS (see the legend for Fig. 10).

Cross-linking—For cross-linking, assembly intermediates of Gag were dialyzed against phosphate-buffered saline (pH 8.0) (for cross-linking with DSP) or 0.2 M triethanolamine (pH 8.0) (for cross-linking with DTBP). DSP or DTBP was added to a final concentration of 1 mM, and the mixtures were incubated at room temperature for 30 min. After quenching with 50 mM Tris (pH 8.0), the materials were dialyzed in buffer A and subjected to *in vitro* assembly reactions at 37 °C for 3 h.

Gradient Analysis—Protein was applied onto a 15–35% (w/v) sucrose gradient and sedimented in an SW55 rotor (Beckman Coulter) at 150,000 × *g* for 4 h at 4 °C. Alternatively, the protein sample was applied onto a 20–70% (w/v) sucrose gradient and sedimented in an SW55 rotor at 120,000 × *g* for 2 h at 4 °C. After centrifugation, the gradients were fractionated from the bottom to the top. A high molecular mass calibration kit (Amersham Biosciences), 80 S ribosome, and the immature form of HIV Gag VLPs purified from the supernatant of Gag-expressing *Sf*9 cells were used for molecular mass markers for sedimentation analyses.

Treatment with Detergent and Urea—Assembly intermediates of Gag were treated with 0.5% Triton X-100, 0.1 or 1.0% sodium deoxycholate, 0.1% SDS, or 6 M urea at room temperature for 15 min. Following treatment, the materials were centrifuged in an SW55 rotor at 220,000 × *g* for 4 h at 4 °C. As a control, the immature form of HIV Gag VLP purified from the supernatant of Gag-expressing *Sf*9 cells was similarly treated with the detergents or urea.

Protein Detection—Proteins were separated by SDS-PAGE and detected by Coomassie Brilliant Blue or silver staining or subjected to Western blotting using anti-HIV-1 CA monoclonal antibody.

Electron Microscopic Examination—Electron microscopic examination was carried out by the standard procedures. Assembly intermediates were collected by centrifugation in an SW55 rotor at 220,000 × *g* for 4 h at 4 °C and fixed with 2% glutaraldehyde and subsequently with 1% osmium tetroxide. Ultrathin sections were stained with uranyl acetate and lead citrate.

RESULTS

Time Courses of HIV Gag Expression and Assembly in E. coli—The HIV-1 *gag* gene with the additional sequence encoding 6 histidine residues at the C terminus was cloned into pTrcHisA vector and used for Gag expression in *E. coli* cells, as described previously (26). *E. coli* was grown at 37 and 30 °C, and protein expression was induced by the addition of IPTG. To monitor Gag expression, whole cell lysates were prepared at 1-, 2-, and 4-h time points following IPTG induction and subjected to SDS-PAGE followed by Coomassie Brilliant Blue staining (Fig. 1, *upper*) and Western blotting with anti-HIV-1 CA antibody (Fig. 1, *lower*). The levels of Gag expression were broadly equivalent with similar kinetics between the two temperatures (Fig. 1, *whole cells*). However, when the cell lysates were subjected to subcellular fractionation by centrifugation at 15,000 × *g* for 30 min, striking differences were observed between the two temperatures. In the 37 °C samples, Gag antigens were initially found in the supernatant but recovered in the pellets after 2 h of induction (Fig. 1, *left*). In contrast, when *E. coli* was maintained at 30 °C, Gags were constantly recovered in the

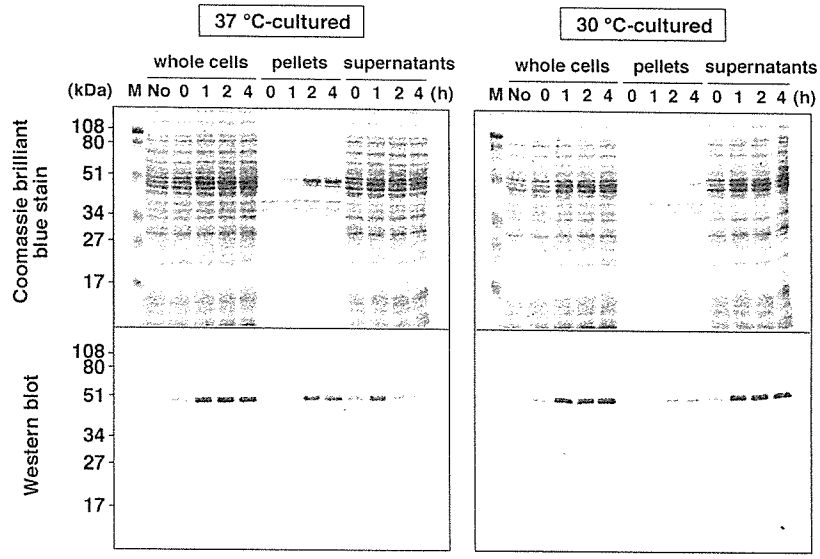

FIG. 1. **Time courses of Gag expression in *E. coli*.** *E. coli* was grown at 37 °C (*left panels*) and 30 °C (*right panels*). Following the addition of IPTG, cells were harvested at intervals. The cells were resuspended in 50 mM Tris (pH 8.0), 150 mM NaCl, 5 mM EDTA, and 1 mM dithiothreitol and disrupted by sonication. Subcellular fractionation was carried out by centrifugation at 15,000 × *g* for 30 min. Equal proportions of the whole cell lysates, the pellets, and the supernatants were analyzed by SDS-PAGE followed by Coomassie Brilliant Blue staining (*upper panels*) and Western blotting using anti-HIV-1 CA antibody (*lower panels*). The lanes are as follows: *M*, prestained molecular mass markers; *No*, *E. coli* transformed with a parental expression vector pTrcHisA; *0–4*, *E. coli* transformed with the HIV-1 *gag* gene-containing vector. *0* shows before induction, and *1*, *2*, and *4* show h after induction, respectively.

supernatants throughout the period observed here (up to 4 h) (Fig. 1*B*). It has been reported for Mason-Pfizer monkey virus that Gag assembles to spherical particles in *E. coli* and forms inclusion bodies, which were precipitated by centrifugation under similar conditions (28).

To examine whether the temperature-dependent differences may represent the assembly state of the expressed Gag protein, sedimentation experiments using sucrose gradients were carried out. Whole cell lysates made at each time point were clarified by brief centrifugation at 1,000 × *g* for 3 min and then sedimented through 20–70% sucrose gradients at 120,000 × *g* for 2 h. Gag antigens spread within the gradients were detected by Western blotting. When the 37 °C samples were analyzed, a progression of Gag toward heavier gradient fractions was apparent with increasing incubation times (Fig. 2A, *left*). Gag antigens were initially found at the top of the gradient but, at 2 h after induction, sedimented to 50% sucrose fractions with a trace of Gag in the 25–30% sucrose fractions. By 4 h, the mobility shift to 50% sucrose fractions was largely complete. In contrast, when *E. coli* was maintained at 30 °C, Gag antigens were initially found at the top of the gradient and later shifted to the 25–30% sucrose fractions but not to the 50% sucrose fractions (Fig. 2A, *right*). These data show that at 37 °C, synthesized Gag forms a large complex from relatively small molecular weight complexes, whereas in contrast, at 30 °C, Gag remains in relatively small complexes.

Electron microscopy was carried out to examine whether the Gag complexes identified by gradient analysis had defined structures. Doughnut-like particles, typical of the immature form of Gag capsids, were observed in the *E. coli* cells maintained at 37 °C (Fig. 2*B*, *left*), confirming previous reports in which retroviral Gag protein (*e.g.* Mason-Pfizer monkey virus, Rous sarcoma virus, and HIV) assemble into VLPs inside *E. coli* cells (24, 27, 28). In contrast, no particles were seen in *E. coli* cells when maintained at 30 °C (Fig. 2*B*, *right*).

Sedimentation Profiles of Assembly Intermediates—To enrich the small complex form of Gag, *E. coli* cells were harvested at each time point after IPTG induction, and Gags were purified from the supernatants of the cell lysates by use of the Gag C-terminal polyhistidine tag. Following metal chelate chromatography, the eluted fractions were analyzed by SDS-PAGE followed by Coomassie Brilliant Blue staining (Fig. 3, *upper*) and Western blotting with anti-HIV-1 CA antibody (Fig. 3, *lower*). When the *E. coli* cells were maintained at 30 °C, Gag could be purified at all time points after induction. In contrast, at 37 °C, Gag was purified only at 1 h but not at any later time points. As Gag forms a large complex with increasing incubation times in 37 °C-cultured *E. coli*, the purification failure is consistent with the inaccessibility of the polyhistidine tag to the metal chelate resin.

Each purified Gag was directly subjected to sedimentation analysis on 20–70% sucrose gradients, and fractions were analyzed by SDS-PAGE followed by silver staining (Fig. 4, *left*). When the 1-h samples were analyzed, both Gags (purified from 37- and 30 °C-cultured *E. coli*) were found at the top of the gradient (Fig. 4, *left*, *37 °C, 1 h* and *30 °C, 1 h*). In contrast, the 4-h sample (purified from 30 °C-cultured *E. coli*) sedimented to 25–30% sucrose fractions (Fig. 4, *left*, *30 °C, 4 h*), showing that by 4 h after induction, Gag forms a small complex that could still be purified by chromatography. The molecular mass of the small Gag complex was determined by subsequent sedimentation analysis on 15–35% sucrose gradients (Fig. 4, *right*). When compared with molecular mass markers and 80 S ribosomes sedimented in parallel, the small Gag complex was detected in fractions corresponding to 60 S (Fig. 4, *right*, *30 °C, 4 h*), whereas the Gags of 1-h samples were detected in much lower molecular mass fractions (Fig. 4, *right*, *37 °C, 1 h* and *30 °C, 1 h*) corresponding to the monomeric form of Gag observed in our previous studies (26).

A number of studies have demonstrated that *in vitro* assembly using purified Gag forms spherical particles, remarkably similar to the immature form of retroviral capsids (25, 27, 28). We have also shown that, in an *in vitro* assembly reaction, Gag forms a 60 S multimer that subsequently shifts to 600 S, equivalent to the immature form of HIV capsids, suggesting that the 60 S multimer may represent an assembly intermediate during capsid formation (26). As expression in *E. coli* cells at 37 °C allowed the production of both large and small Gag complexes, but at 30 °C, allowed only the small complex (Fig. 2), we tested whether Gag assembly *in vitro* is similarly tem-

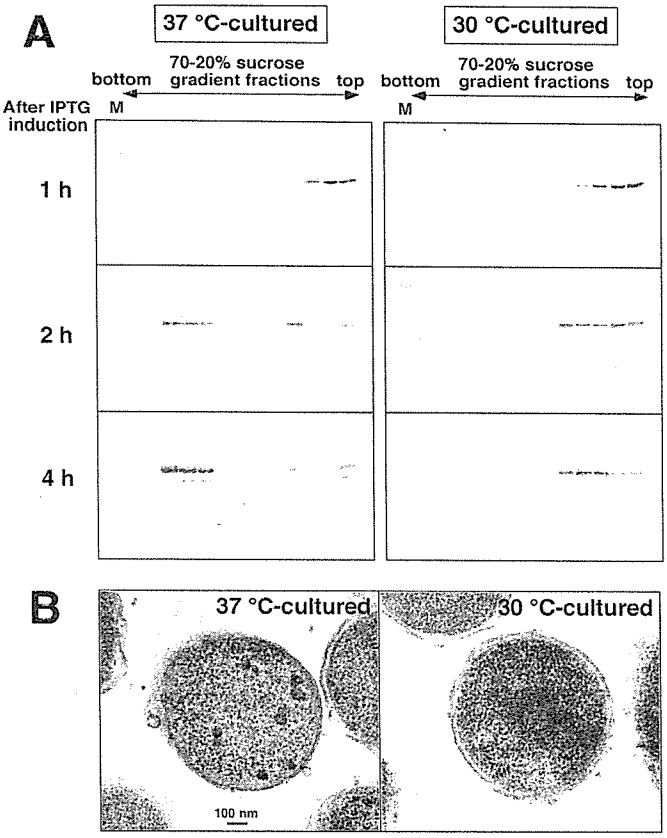

FIG. 2. **Time courses of Gag assembly in *E. coli*.** *A*, gradient analysis of the whole cell lysates of *E. coli*. *E. coli* was grown at 37 °C (*left panels*) and 30 °C (*right panels*) and, after IPTG induction, the cells were harvested at intervals. The whole cell lysates were prepared as described in the legend for Fig. 1 and then incubated with 10 μg/ml RNaseA for 10 min. Following clarification by brief centrifugation at 1,000 × *g* for 3 min, the lysates were applied on 20–70% (w/v) sucrose gradients and centrifuged at 120,000 × *g* for 2 h at 4 °C. Gradient fractions from the *bottom* to the *top* (*left* to *right*) were analyzed by Western blotting using anti-HIV-1 CA antibody. *Lane M* shows prestained molecular mass markers. *B*, electron microscopy of *E. coli* cells. After 4 h of IPTG induction, *E. coli* cells were collected and subjected to electron microscopic analysis. *Scale bars* represent 100 nm.

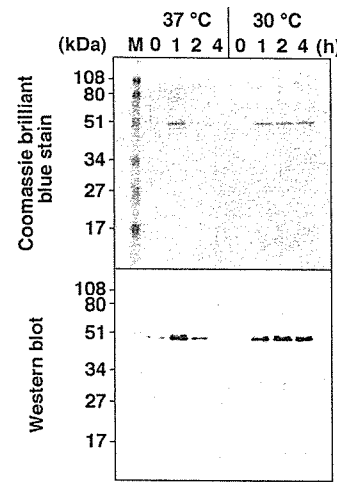

FIG. 3. **Purification of Gag protein.** *E. coli* was grown at 37 and 30 °C. Following the addition of IPTG, cells were harvested at intervals. For metal chelate chromatography, the cells were resuspended in 20 mM Tris (pH 7.9), 150 mM NaCl, and 10 mM imidazole. Following sonication at 4 °C for 15 min, the cells were lysed by 0.1% Nonidet P-40 and incubated at room temperature for 10 min in the presence of 10 μg/ml RNaseA. The cell lysates were clarified by centrifugation at 4 °C at 15,000 × *g* for 30 min, and the supernatants were subjected to metal chelate chromatography. Eluted fractions were analyzed by SDS-PAGE followed by Coomassie Brilliant Blue staining (*upper panel*) and Western blotting using anti-HIV-1 CA antibody (*lower panel*). The lanes are as follows: *M*, prestained molecular mass markers; *0*, purified from *E. coli* before IPTG induction; *1*, *2*, and *4*; purified from *E. coli* after 1, 2, and 4 h of IPTG induction, respectively.

perature-dependent. Monomeric Gag was purified following 1 h of IPTG induction and subjected to the *in vitro* assembly reaction described previously (26). The *in vitro* assembly products were analyzed on 20–70% sucrose gradients and compared with 80 S ribosomes and the immature form of HIV capsids sedimented in parallel. When the *in vitro* assembly reaction was carried out at 30 °C, Gag, whether derived from *E. coli* cultured at 37 or 30 °C, sedimented to a position corresponding to 60 S (Fig. 5, *middle*). In contrast, when the reaction was carried out at 37 °C, the sedimentation profiles for both Gags were shifted essentially to that of the immature form of Gag capsids, although a small fraction of Gag was still observed at 60 S (Fig. 5, *bottom*). These data indicate that, in our *in vitro* assembly system, the 30 °C reaction produces only 60 S Gag multimers and that higher order assembly requires incubation at 37 °C, paralleling the Gag assembly observed in *E. coli* cells. The data from the *in vitro* system also show that the levels of Gag assembly were dependent on the temperatures of the *in vitro* reaction but not on the temperatures at which the Gags were purified from *E. coli*.

Morphology of Assembly Intermediates—Electron microscopic examination was used to examine whether the 60 S Gag complex had a defined structure. *E. coli*-produced 60 S complex was purified by metal chelate chromatography from *E. coli* following 4 h of IPTG induction at 30 °C, and *in vitro*-assembled 60 S complex was prepared by *in vitro* reaction at 30 °C for 3 h using purified monomeric Gag protein. When observed by ultrathin section transmission microscopy, the *E. coli*-produced 60 S complex did not exhibit doughnut-like structures but rather exhibited crescent-shaped structures with double electron-dense layers. The structures very often resembled small patches of electron-dense materials observed under the plasma membrane of Gag-expressing eukaryotic cells (Fig. 6*A*). The *in vitro*-assembled 60 S complex showed a similar structure. The complex formed electron-dense structures with a gentle curvature, although the contours of the structures were not as sharp when compared with the 60 S complex produced from *E. coli* (Fig. 6*B*), suggesting that Gag-Gag interaction may be somewhat weaker following the *in vitro* assembly reaction. For comparison, we enriched the large Gag complex, corresponding to 600 S, which was observed in *E. coli* cells (Fig. 2, *left*) as described previously (28). As expected, the structure of the complex showed a hollow sphere surrounded by a double ring structure (Fig. 6*C*), typical of the immature form of Gag capsids. These data support the conjecture that the 60 S Gag complex observed in this work may represent a distinct assembly intermediate formed during the process of Gag assembly. The data also suggest that the formation of Gag capsids is not initiated by random accumulation of Gag proteins but rather by an ordered arrangement of Gag molecules following a defined assembly pathway.

Detergent Resistance of Assembly Intermediates—It has been reported that the immature forms of retroviral capsids remain intact following treatment with nonionic detergents such as Triton X-100 and Nonidet P-40 (34, 35) but are dissociated by SDS and urea. Accordingly, the detergent resistance of the 60 S Gag complexes observed here was examined to reveal the similarities with completely assembled Gag capsids. As the 60 S Gag complexes, whether *E. coli*-produced or *in vitro*-assembled, were wholly pelleted by centrifugation at 220,000 × *g* for 4 h (Fig. 7*A*), the centrifugation conditions were used for an analysis of the effect of detergent treatment. Irrespective of

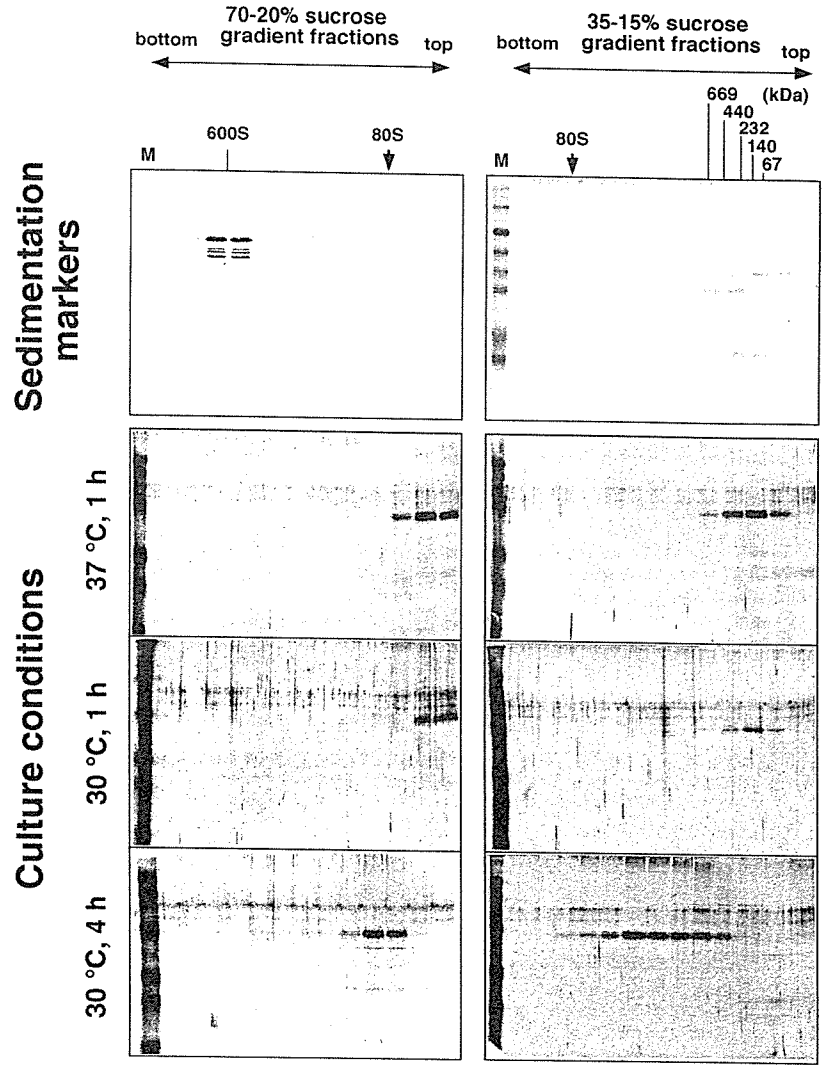

FIG. 4. **Gradient analysis of Gag assembly intermediates produced in *E. coli*.** Expression and purification of Gag were carried out as described in the legend for Fig. 3. The Gag protein purified after 1 or 4 h of induction was analyzed on 20–70% (w/v) sucrose gradients by centrifugation at 120,000 × *g* for 2 h (*right panels*) and on 15–35% (w/v) sucrose gradients by centrifugation at 150,000 × *g* for 4 h (*left panels*). Gradient fractions were subjected to SDS-PAGE followed by silver staining. Sedimentation markers are as follows: the immature form of HIV capsids (600 S) detected by Western blotting (*left top panel*); high molecular mass calibration markers consisting of thyroglobulin (669 kDa = 2 × 330 kDa), ferritin (440 kDa = 2 × 220 kDa), catalase (232 kDa = 4 × 60 kDa), lactate dehydrogenase (140 kDa = 4 × 36 kDa), and albumin (67 kDa) (Amersham Biosciences), stained with Coomassie Brilliant Blue (*right top panel*). *Arrows* on the *top panels* show a sedimented position of 80 S ribosomes. *Lane M* shows prestained molecular mass markers for SDS-PAGE.

their origin, the 60 S Gag complexes were not dissociated by treatment with 0.5% Triton X-100, mimicking the stability of the immature form of HIV capsids in the presence of the detergent. In contrast, when treated with 6 M urea or 0.1% SDS, the complexes dissociated completely, as was also observed with the immature form of Gag capsids. Differences were observed when the materials were treated with 0.1% sodium deoxycholate, however. The immature forms of Gag capsids were partially dissociated by the treatment, whereas in contrast, the 60 S forms of Gag complexes were completely dissociated (Fig. 7*B*). Treatment with 1% sodium deoxycholate led to complete dissociation of the immature form of Gag capsids (data not shown).

Mechanisms of Assembly—Our *in vitro* assembly reactions suggest that incubation at 37 °C was solely responsible for the formation of a high order of Gag multimer (Fig. 5). A simple interpretation of the data would be that Gag conformation might be altered or that Gag-Gag interactions might be stimulated at 37 °C. To test these possibilities, the 60 S Gag multimers were cross-linked, not to allow large conformational changes but possibly to allow multimer-multimer interactions in subsequent *in vitro* assembly reactions, and then subjected to sedimentation analysis on 20–70% sucrose gradients. When the 60 S Gag multimer was cross-linked with DSP, the *in vitro* reaction at 37 °C did not produce any higher order of multimers (Fig. 8, *upper middle*). A similar finding was observed when DTBP, an imidoester cross-linker potentially retaining the native conformation of protein, was used (Fig. 8, *lower middle*). These data suggest that Gag conformational changes may be required for higher order assembly, although it cannot be ruled out that unwanted side chains introduced by the cross-linkers might inhibit multimer-multimer interactions. As glycerol is known to stabilize protein conformation, we also tested the effect of glycerol on Gag assembly. *In vitro* assembly reactions with the 60 S Gag multimers in the presence of 10% (v/v) glycerol, even when carried out at 37 °C, did not produce any higher order of multimers (Fig. 8, *bottom*), suggesting that stabilization of the multimers may have an inhibitory effect on the higher order of Gag multimerization. Alternatively, exposure to glycerol, a hydrogen donor, might lead to weakening the hydrogen bonds possibly formed by higher order assembly. It is unlikely that the addition of glycerol might cause an increase in the solution viscosity, leading to a reduction in protein mobility, because our *in vitro* reactions were carried out at 37 °C, a relatively high temperature.

Some recent studies have suggested that retroviral Gag assembly is energy-dependent (36–38). It is possible that the Gag assembly in *E. coli* cells observed in this study might occur in an energy-dependent manner but not simply in a temperature-dependent manner. To this end, NaN_3, which has been shown to deplete cellular ATP from *E. coli* (32, 33), was added at a range of 0–10 mM to the culture medium following IPTG addition, and *E. coli* was cultured at 37 °C for 4 h, conditions under which the majority of Gag normally assembles up to 600 S. Western blotting of whole cell lysates revealed near equivalent levels of Gag expression up to 5 mM NaN_3, suggesting little

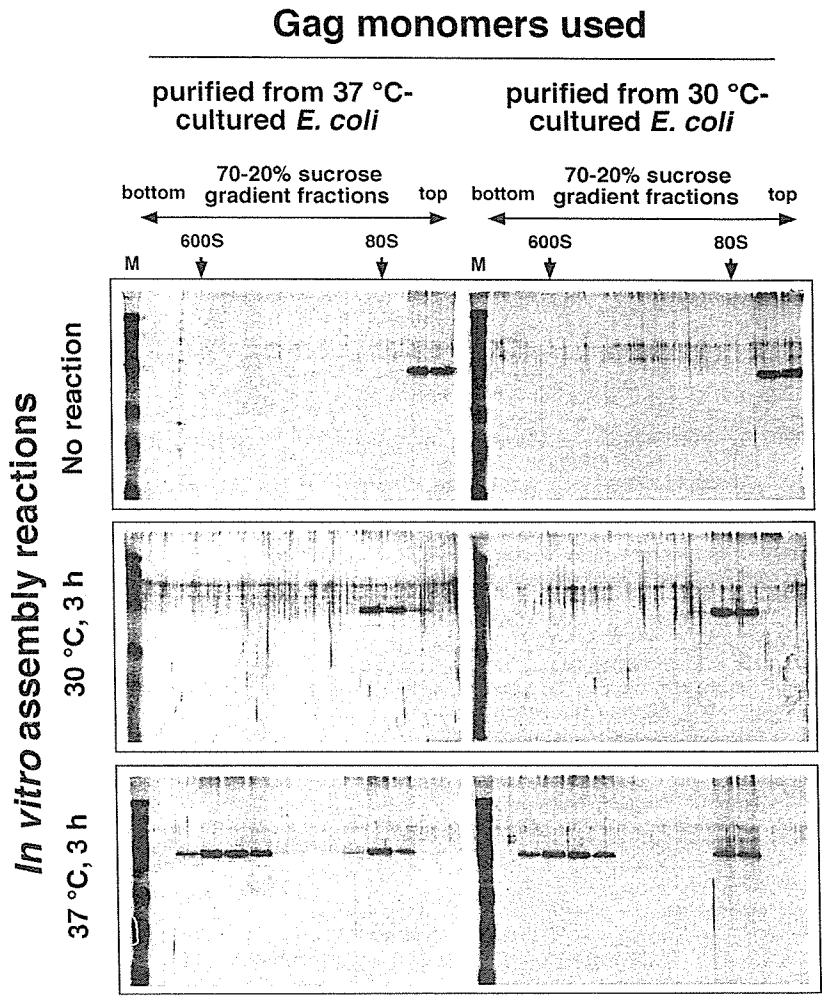

FIG. 5. **Gradient analysis of Gag assembly intermediates produced by *in vitro* assembly reaction.** *E. coli* was cultured at 37 and 30 °C and, after 1 h of IPTG induction, Gag protein was purified by metal chelate chromatography as described in the legend for Fig. 3. Eluted fractions were desalted using Sephadex G-25 (PD-10) equilibrated with buffer A (20 mM Tris (pH 8.6 adjusted at room temperature), 100 mM NaCl, 0.2 mM EDTA, 5 mM $MgCl_2$, and 1 mM dithiothreitol). For *in vitro* assembly, the fractions were incubated at 30 °C (*middle panels*) or 37 °C (*bottom panels*) for 3 h. The products were applied on 20–70% (w/v) sucrose gradients and centrifuged at 120,000 × *g* for 2 h at 4 °C. Gradient fractions from the *bottom* to the *top* (*left* to *right*) were analyzed by SDS-PAGE followed by silver staining. *In vitro* assembly reaction was carried out using monomeric Gag protein purified from 37 °C-cultured *E. coli* (*left panels*) and using monomeric Gag protein purified from 30 °C-cultured *E. coli* (*right panels*). *Arrows* show sedimented positions of the immature form of HIV capsids (600 S) and 80 S ribosomes. *Lane M* shows prestained molecular mass markers for SDS-PAGE.

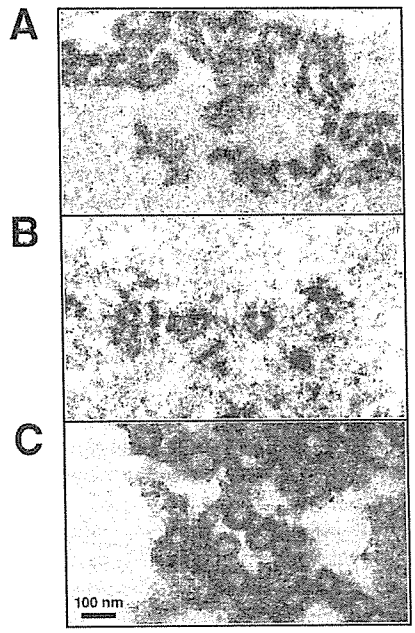

FIG. 6. **Electron microscopy of Gag assembly intermediates.** *E. coli*-produced 60 S complex was purified from *E. coli* following 4 h of induction at 30 °C (*A*), and *in vitro*-assembled 60 S complex was prepared by *in vitro* reaction at 30 °C for 3 h (*B*). For comparison, *E. coli*-produced 600 S complex, similar to the immature form of authentic Gag capsids, was purified as described previously (28) (*C*). The materials were observed by ultrathin section transmission. *Scale bars* represent 100 nm.

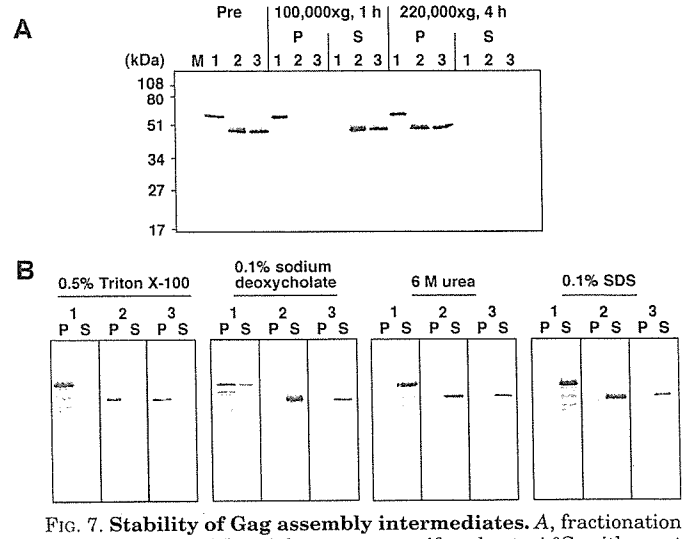

FIG. 7. **Stability of Gag assembly intermediates.** *A*, fractionation by centrifugation. Materials were centrifuged at 4 °C either at 120,000 × *g* for 1 h or at 220,000 × *g* for 4 h. The pellets (*P*) and supernatants (*S*) were analyzed by SDS-PAGE followed by Western blotting using anti-HIV-1 CA antibody. *Pre* shows materials before centrifugation. *B*, fractionation following detergent/urea treatment. Materials were treated with 0.5% Triton X-100, 0.1% sodium deoxycholate, 6 M urea, or 0.1% SDS and subjected to centrifugation at 220,000 × *g* for 4 h. Following fractionation into pellets and supernatants, Gag antigens were similarly detected by Western blotting. Materials are as follows: *1*, the immature form of HIV capsids; *2*, *E. coli*-produced 60 S complex; *3*, *in vitro*-assembled 60 S complex. *Lane M* shows prestained molecular mass markers.

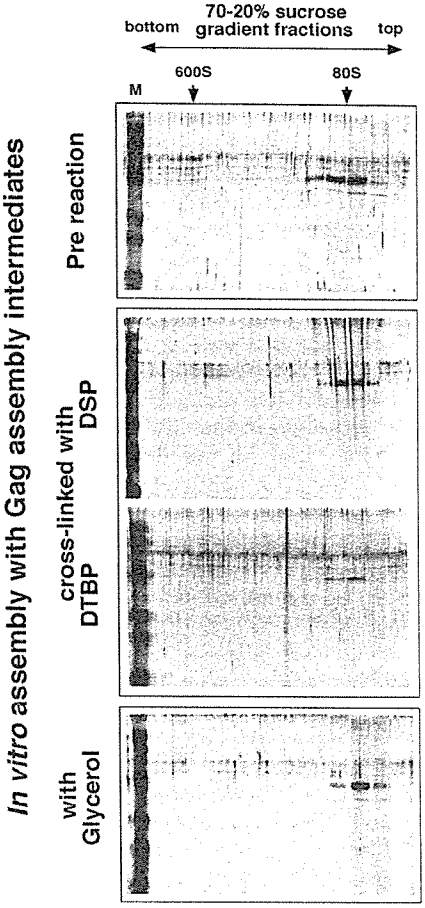

FIG. 8. **Effect of cross-linking and glycerol on higher order assembly.** Gag assembly intermediates were incubated with DSP (*upper middle panel*) or DTBP (*lower middle panel*) at room temperature for 30 min. For the higher order of assembly, the materials were dialyzed in buffer A (as described in the legend for Fig. 5) and incubated at 37 °C for 3 h. Alternatively, Gag assembly intermediates were incubated at 37 °C for 3 h in the presence of 10% (v/v) glycerol (*bottom panel*). The products were analyzed on 20–70% (w/v) sucrose gradients by centrifugation at 120,000 × *g* for 2 h at 4 °C. Gradient fractions from the *bottom* to the *top* (*left* to *right*) were subjected to SDS-PAGE followed by silver staining. *Arrows* show sedimented positions of the immature form of HIV capsids (600 S) and 80 S ribosomes. *Lane M* shows prestained molecular mass markers for SDS-PAGE.

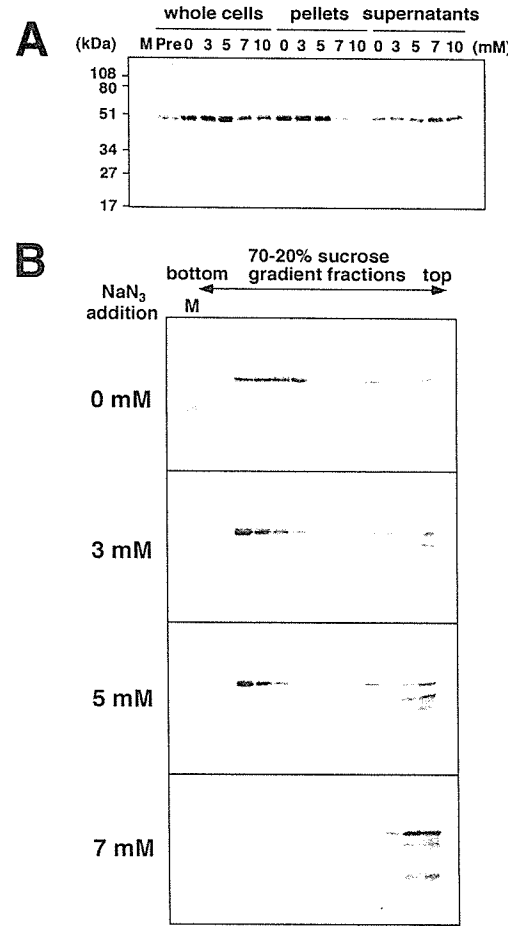

FIG. 9. **Gag assembly in *E. coli* treated with NaN_3.** *A*, subcellular fractionation of *E. coli*. Following the addition of IPTG and subsequently NaN_3, *E. coli* was grown at 37 °C for 4 h. Cell harvest and subcellular fractionation were carried out as described in the legend for Fig. 1. Equal proportions of the whole cell lysates, the pellets, and the supernatants were analyzed by SDS-PAGE followed by Western blotting using anti-HIV-1 CA antibody. The lanes are as follows: *M*, prestained molecular mass markers; *Pre*, before induction; *0*, *3*, *5*, *7*, and *10*, 4 h after induction. *0*, *3*, *5*, *7*, and *10* show mM NaN_3, respectively. *B*, gradient analysis of the whole cell lysates of *E. coli*. The whole cell lysates prepared as described above were incubated with 10 μg/ml RNaseA. Following clarification by brief centrifugation, the lysates were analyzed on 20–70% (w/v) sucrose gradients by centrifugation at 120,000 × *g* for 2 h at 4 °C. Gradient fractions from the *bottom* to the *top* (left to *right*) were analyzed by Western blotting using anti-HIV-1 CA antibody. *Lane M* shows prestained molecular mass markers.

effect on Gag synthesis. In contrast, Gag expression was severely impaired when added at 7 mM. When cell lysates were subjected to subcellular fractionation by centrifugation as before, the majority of Gag antigens was recovered in the pellets in the 0–5 mM treatments (Fig. 9*A*). Consistent with this, when whole cell lysates were subjected to sedimentation analysis on 20–70% sucrose gradients, Gag multimerization to the 600 S form appeared unaffected up to 5 mM but was abolished at 7 mM when Gag synthesis was also impaired (Fig. 9*B*). Although we did not measure the intracellular levels of ATP, it is unlikely in this cell system that Gag assembly process is ATP-dependent.

We also tested whether the higher order assembly observed here, although temperature-dependent, could be facilitated with molecular chaperonins. Equimolar GroEL-GroES was added to an *in vitro* assembly reaction with the 60 S Gag multimer, and the mixture was incubated in the presence of 1 mM ATP (or ATP-γS) at 37 °C but only for 1 h, conditions under which Gag alone assembles to 150–350 S but not up to 600 S (26). Sedimentation analysis of the assembly products showed Gag distribution at a broad range of 150–350 S, essentially similar to that obtained by an *in vitro* assembly reaction with the 60 S Gag multimer alone (Fig. 10), indicating that GroEL-GroES did not facilitate Gag assembly. These data suggest that GroEL-GroES may not be capable of refolding of Gag or that the Gag molecule used here has already been folded into assembly-competent forms.

DISCUSSION

Retroviral Gag protein is initially synthesized in the cytosol but undergoes a process of assembly to form a viral particle. Particle assembly must require the ordered multimerization of Gags, and some studies suggest that the formation of assembly intermediates occurs during this process. Crystallographic studies have provided evidence of trimerization by MA (39, 40) and dimerization by CA (30, 41–44), and *in vitro* assembly studies have suggested Gag dimerization through NC-RNA interaction (45). Similar Gag oligomeric forms were observed in Gag-expressing eukaryotic cells (31). These data suggest that the minimum assembly units of Gag are a dimer and a trimer. In contrast, electron microscopic examination has provided clear evidence of only large-sized assembly intermediates, vis-

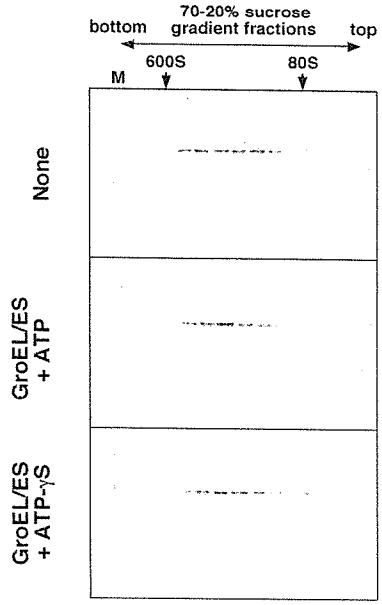

FIG. 10. **Effect of GroEL/GroES on higher order assembly.** Gag assembly intermediates were incubated at 37 °C for 1 h without (*top panel*) or with 0.3–0.5 mg/ml GroEL/GroES in the presence of 1 mM ATP (*middle panel*) or ATP-γS (*bottom panel*). The products were analyzed on 20–70% (w/v) sucrose gradients by centrifugation at 120,000 × *g* for 2 h at 4 °C. Gradient fractions from the *bottom* to the *top* (*left* to *right*) were subjected to SDS-PAGE followed by Western blotting using anti-HIV-1 CA antibody. *Arrows* show sedimented positions of the immature form of HIV capsids (600 S) and 80 S ribosomes. *Lane M* shows prestained molecular mass markers for SDS-PAGE.

ible for C type retroviruses and lentiviruses such as HIV in Gag-expressing cells as electron-dense layers underneath the plasma membrane and membrane projections with nascent Gag capsids (15). These structures are likely to be assembly intermediates at a relatively late stage of the assembly process.

For putative assembly intermediates, we initially used *E. coli* expression systems and noted the appearance of 60 S Gag multimers that subsequently converted to completed 600 S capsids. Consistent with this finding, when the monomeric form of purified Gag was subjected to an *in vitro* assembly reaction, a similar level of Gag multimers formed that also subsequently shifted to 600 S, corresponding to completely assembled products. The data suggest that the 60 S form of Gag multimers is likely to be an assembly intermediate in these assembly systems. No other larger size classes of intermediate were detected in our studies. Although there have been a few reports on the biochemical features of such intermediates, one study has previously shown, by gradient analysis of *in vitro* translation products, discrete size classes of Gag intermediates at 10, 80, and 150 S, which were converted to a final completed capsid product with increasing reaction time (36). Our speculation is that the 80 S complex equates to the 60 S multimer observed in our work, as the S value assignments for both intermediates are very approximate estimates. It should be noted that in our study, the 60 S multimers accumulated when *E. coli* induction and *in vitro* assembly reactions were carried out at 30 °C but not at 37 °C (Figs. 2 and 5). When experiments were carried out at 37 °C, the 60 S multimers were only a transient form and rapidly converted to completely assembled capsids. This means that, in any studies at higher temperatures, Gag assembly occurs more rapidly and completely with the result that assembly intermediates may be more difficult to observe. Interestingly, in the *in vitro* translation experiments in which the formation of the 80 S forms of Gag complex was seen, assembly was carried out at 25 °C (36). Thus, incubation at lower temperatures might be the key factor in the observation of intermediates in both studies.

For biochemical and structural studies of the Gag assembly intermediates, we purified the 60 S Gag complex and carried out experiments on detergent sensitivity and observation by electron microscopy. The stability profiles of the *E. coli*-produced and *in vitro*-assembled 60 S complexes were largely similar to those of the immature form of Gag capsids, suggesting somewhat parallel characteristics between partially assembled Gag products and complete Gag capsids. These suggestions were supported by our electron microscopic observations that both 60 S forms of Gag complexes had defined structures such as opposed electron-dense layers. The data suggest that the process of assembly involves Gag being arranged in order from the beginning of the assembly process rather than being rearranged following random accumulation.

However, the instability of the 60 S Gag multimer in 0.1% sodium deoxycholate and the requirement of incubation at 37 °C for higher order assembly suggest that there may be some structural differences between the 60 S form of Gag multimers and the complete form of Gag capsids. To understand the higher order of Gag assembly, we used cross-linkers so as not to allow Gag conformational changes and found that, once cross-linked, the 60 S Gag multimers did not shift to any higher order forms. These data suggest, although do not prove, that Gag assembly may be accompanied by the conformational changes in Gag induced at 37 °C. A similar *in vitro* assembly study with Rous sarcoma virus Gag protein has suggested that acidic pH triggers conformational changes in Gag, leading to a high order of Gag multimerization such as VLP (46).

Some recent studies have suggested the involvement of ATP-dependent pathways in retroviral Gag assembly (36–38), but the stage at which ATP acts has not been determined. One study in which ATP was depleted from COS-1 cells expressing HIV Gag showed that the blockage occurs at the stage at which the VLPs are pinched off from membrane but not at any earlier stages such as Gag membrane binding and multimerization (37). However, when a similar experiment was carried out with Mason-Pfizer monkey virus Gag, a prototype for capsid formation prior to membrane relocation, the blockage was observed at both stages of capsid assembly and transport (38). Another study in which ATP was depleted from an *in vitro* translation system for the synthesis of HIV Gag showed the blockage at the stage of Gag multimerization, suggesting the involvement of a chaperonin-like host factor (36, 47). These somewhat conflicting data need to be reconciled by further investigation. In our study, neither ATP nor GroEL-GroES, a prokaryotic chaperonin, was required for Gag multimerization, although we cannot rule out the possibility that eukaryotic chaperonins may support Gag multimerization in higher eukaryotic cells. The association of retroviral Gags with eukaryotic chaperonins have recently been reported (47, 48), but it remains to be elucidated whether or not Gags are folded into assembly-competent forms by the chaperonins.

Acknowledgment—We thank Dr. Ian M. Jones (The University of Reading, Reading, UK) for discussions on the manuscript.

REFERENCES

1. Gheysen, D., Jacobs, E., de Foresta, F., Thiriart, C., Francotte, M., Thines, D., and De Wilde, M. (1989) *Cell* **59,** 103–112
2. Hoshikawa, N., Kojima, A., Yasuda, A., Takayashiki, E., Masuko, S., Chiba, J., Sata, T., and Kurata, T. (1991) *J. Gen. Virol.* **72,** 2509–2517
3. Smith, A. J., Srinivasakumar, N., Hammarskjold, M. L., and Rekosh, D. (1993) *J. Virol.* **67,** 2266–2275
4. Bryant, M., and Ratner, L. (1990) *Proc. Natl. Acad. Sci. U. S. A.* **87,** 523–527
5. Gottlinger, H. G., Sodroski, J. G., and Haseltine, W. A. (1989) *Proc. Natl. Acad. Sci. U. S. A.* **86,** 5781–5785
6. Carriere, C., Gay, B., Chazal, N., Morin, N., and Boulanger, P. (1995) *J. Virol.* **69,** 2366–2377
7. Dorfman, T., Bukovsky, A., Ohagen, A., Hoglund, S., and Gottlinger, H. G. (1994) *J. Virol.* **68,** 8180–8187

8. Mammano, F., Ohagen, A., Hoglund, S., and Gottlinger, H. G. (1994) *J. Virol.* **68,** 4927–4936
9. Reicin, A. S., Paik, S., Berkowitz, R. D., Luban, J., Lowy, I., and Goff, S. P. (1995) *J. Virol.* **69,** 642–650
10. Gottlinger, H. G., Dorfman, T., Sodroski, J. G., and Haseltine, W. A. (1991) *Proc. Natl. Acad. Sci. U. S. A.* **88,** 3195–3199
11. Parent, L. J., Bennett, R. P., Craven, R. C., Nelle, T. D., Krishna, N. K., Bowzard, J. B., Wilson, C. B., Puffer, B. A., Montelaro, R. C., and Wills, J. W. (1995) *J. Virol.* **69,** 5455–5460
12. Forster, M. J., Mulloy, B., and Nermut, M. V. (2000) *J. Mol. Biol.* **298,** 841–857
13. Fuller, S. D., Wilk, T., Gowen, B. E., Krausslich, H. G., and Vogt, V. M. (1997) *Curr. Biol.* **7,** 729–738
14. Nermut, M. V., Hockley, D. J., Jowett, J. B., Jones, I. M., Garreau, M., and Thomas, D. (1994) *Virology* **198,** 288–296
15. Gelderblom, H. R. (1991) *AIDS* **5,** 617–638
16. Tritel, M., and Resh, M. D. (2000) *J. Virol.* **74,** 5845–5855
17. Perrin-Tricaud, C., Davoust, J., and Jones, I. M. (1999) *Virology* **255,** 20–25
18. Wang, J. J., Sandefur, S., Spearman, P., Chiou, C. T., Chiang, P. H., and Ratner, L. (2001) *Appl. Immunohistochem. Mol. Morphol.* **9,** 371–379
19. Lee, Y. M., and Yu, X. F. (1998) *Virology* **243,** 78–93
20. Lee, Y. M., Liu, B., and Yu, X. F. (1999) *J. Virol.* **73,** 5654–5662
21. Nermut, M. V., Zhang, W.-H., Francis, G., Ciamporx, F., Morikawa, Y., and Jones, I. M. (2003) *Virology* **305,** 219–227
22. Duronio, R. J., Jackson-Machelski, E., Heuckeroth, R. O., Olins, P. O., Devine, C. S., Yonemoto, W., Slice, L. W., Taylor, S. S., and Gordon, J. I. (1990) *Proc. Natl. Acad. Sci. U. S. A.* **87,** 1506–1510
23. Morikawa, Y., Kinoshita, A., Goto, T., Tomoda, H., and Sano, K. (2001) *Virology* **283,** 343–352
24. Gross, I., Hohenberg, H., Huckhagel, C., and Krausslich, H. G. (1998) *J. Virol.* **72,** 4798–4810
25. Campbell, S., and Rein, A. (1999) *J. Virol.* **73,** 2270–2279
26. Morikawa, Y., Goto, T., and Sano, K. (1999) *J. Biol. Chem.* **274,** 27997–28002
27. Campbell, S., and Vogt, V. M. (1997) *J. Virol.* **71,** 4425–4435
28. Klikova, M., Rhee, S. S., Hunter, E., and Ruml, T. (1995) *J. Virol.* **69,** 1093–1098
29. Ganser, B. K., Li, S., Klishko, V. Y., Finch, J. T., and Sundquist, W. I. (1999) *Science* **283,** 80–83
30. von Schwedler, U. K., Stemmler, T. L., Klishko, V. Y., Li, S., Albertine, K. H., Davis, D. R., and Sundquist, W. I. (1998) *EMBO J.* **17,** 1555–1568
31. Morikawa, Y., Hockley, D. J., Nermut, M. V., and Jones, I. M. (2000) *J. Virol.* **74,** 16–23
32. Kihara, A., and Ito, K. (1998) *J. Biol. Chem.* **45,** 19770–19775
33. van der Wolk, J. P., de Wit, J. G., and Driessen, A. J. (1997) *EMBO J.* **16,** 7297–7304
34. Rose, J. R., Babe, L. M., and Craik, C. S. (1995) *J. Virol.* **69,** 2751–2758
35. Stewart, L., Schatz, G., and Vogt, V. M. (1990) *J. Virol.* **64,** 5076–5092
36. Lingappa, J. R., Hill, R. L., Wong, M. L., and Hegde, R. S. (1997) *J. Cell Biol.* **136,** 567–581
37. Tritel, M., and Resh, M. D. (2001) *J. Virol.* **75,** 5473–5481
38. Weldon, R. A., Jr., Parker, W. B., Sakalian, M., and Hunter, E. (1998) *J. Virol.* **72,** 3098–3106
39. Hill, C. P., Worthylake, D., Bancroft, D. P., Christensen, A. M., and Sundquist, W. I. (1996) *Proc. Natl. Acad. Sci. U. S. A.* **93,** 3099–3104
40. Rao, Z., Belyaev, A. S., Fry, E., Roy, P., Jones, I. M., and Stuart, D. I. (1995) *Nature* **378,** 743–747
41. Berthet-Colominas, C., Monaco, S., Novelli, A., Sibai, G., Mallet, F., and Cusack, S. (1999) *EMBO J.* **18,** 1124–1136
42. Gamble, T. R., Vajdos, F. F., Yoo, S., Worthylake, D. K., Houseweart, M., Sundquist, W. I., and Hill, C. P. (1996) *Cell* **87,** 1285–1294
43. Gamble, T. R., Yoo, S., Vajdos, F. F., von Schwedler, U. K., Worthylake, D. K., Wang, H., McCutcheon, J. P., Sundquist, W. I., and Hill, C. P. (1997) *Science* **278,** 849–853
44. Momany, C., Kovari, L. C., Prongay, A. J., Keller, W., Gitti, R. K., Lee, B. M., Gorbalenya, A. E., Tong, L., McClure, J., Ehrlich, L. S., Summers, M. F., Carter, C., and Rossmann, M. G. (1996) *Nat. Struct. Biol.* **3,** 763–770
45. Ma, Y. M., and Vogt, V. M. (2002) *J. Virol.* **76,** 5452–5462
46. Ma, Y. M., and Vogt, V. M. (2004) *J. Virol.* **78,** 52–60
47. Zimmerman, C., Klein, K. C., Kiser, P. K., Singh, A. R., Firestein, B. L., Riba, S. C., and Lingappa, J. R. (2002) *Nature* **415,** 88–92
48. Hong, S., Choi, G., Park, S., Chung, A. S., Hunter, E., and Rhee, S. S. (2001) *J. Virol.* **75,** 2526–2534

Available online at www.sciencedirect.com
ScienceDirect
Microbes and Infection 8 (2006) 2736–2744
Microbes and Infection
www.elsevier.com/locate/micinf

Original article

HIV-1 Vpr induces G2 cell cycle arrest in fission yeast associated with Rad24/14-3-3-dependent, Chk1/Cds1-independent Wee1 upregulation

Naoto Matsuda [a], Hiroko Tanaka [a], Sanae Yamazaki [a], Jun-ichiro Suzuki [a], Koichi Tanaka [b], Takeshi Yamada [c], Michiaki Masuda [a,*]

[a] *Department of Microbiology, Dokkyo Medical University School of Medicine, Kita-kobayashi 880, Mibu, Tochigi 321-0293, Japan*
[b] *Department of Molecular Biology, Graduate School of Medicine, The University of Tokyo, Tokyo 113-0033, Japan*
[c] *Department of Microbiology, Graduate School of Medicine, The University of Tokyo, Tokyo 113-0033, Japan*

Received 23 May 2006; accepted 7 August 2006
Available online 30 August 2006

Abstract

Viral protein R (Vpr), an accessory protein of human immunodeficiency virus type 1 (HIV-1), induces the G2 cell cycle arrest in fission yeast for which host factors, such as Wee1 and Rad24, are required. Catalyzing the inhibitory phosphorylation of Cdc2, Wee1 is known to serve as a major regulator of G2/M transition in the eukaryotic cell cycle. It has been reported that the G2 checkpoint induced by DNA damage or incomplete DNA replication is associated with phosphorylation and upregulation of Wee1 for which Chk1 and Cds1 kinase is required. In this study, we demonstrate that the G2 arrest induced by HIV-1 Vpr in fission yeast is also associated with increase in the phosphorylation and amount of Wee1, but in a Chk1/Cds1-independent manner. Rad24 and human 14-3-3 appear to contribute to Vpr-induced G2 arrest by elevating the level of Wee1 expression. It appears that Vpr could cause the G2 arrest through a mechanism similar to, but distinct from, the physiological G2 checkpoint controls. The results may provide useful insights into the mechanism by which HIV-1 Vpr causes the G2 arrest in eukaryotic cells. Vpr may also serve as a useful molecular tool for exploring novel cell cycle control mechanisms.

Keywords: HIV-1; Vpr; Cell cycle; Fission yeast; Wee1; Chk1; Cds1; Rad24; 14-3-3

1. Introduction

Viral protein R (Vpr) is an accessory protein encoded by human immunodeficiency virus type 1 (HIV-1), which causes acquired immunodeficiency syndrome. It has been shown that Vpr arrests cell cycling at the G2/M boundary in various mammalian cells [1–3]. The ability of Vpr to induce G2 arrest is conserved among primate lentiviruses including HIV-2 and simian immunodeficiency viruses [4], suggesting that it may play important roles in viral replication, such as activation of transcription from the HIV-1 long terminal repeat [5]. Interestingly, Vpr also causes G2 arrest in the fission yeast *Schizosaccharomyces pombe* [6–8]. Our previous studies demonstrated that *wee1* and *rad24* mutants of *S. pombe* were refractory to Vpr-induced G2 arrest, indicating that cellular genes, such as $wee1^+$ and $rad24^+$, were necessary for G2 arrest induction by Vpr in *S. pombe* [8].

A number of genes encoding cell cycle regulatory molecules have been identified using the fission yeast *Schizosaccharomyces pombe*, which serves as a useful model organism for higher eukaryotes including human. Among these genes, $wee1^+$ was originally defined from genetic analysis of *S. pombe* mutants

* Corresponding author. Tel.: +81 282 872131; fax: +81 282 865616.
E-mail address: m-masuda@dokkyomed.ac.jp (M. Masuda).

1286-4579/$ - see front matter © 2006 Elsevier Masson SAS. All rights reserved.
doi:10.1016/j.micinf.2006.08.003

that underwent cell division at a reduced cell size (*wee* phenotype) as a gene regulating the timing of mitosis [9]. Additional studies indicated that Wee1 negatively regulates Cdc2, which plays an essential role in G2/M transition of the cell cycle, through phosphorylation of tyrosine-15 (Y15) of Cdc2 [10]. Discovery of Cdc25 protein phosphatase, which dephosphorylates Y15 of Cdc2, has led to a general understanding that relative activities of Wee1 and Cdc25 are crucial determinants for the timing of G2/M transition in normal cell cycle progression and G2 checkpoint controls [11]. Wee1 activity appears to be controlled through multiple mechanisms, depending on the molecular events that affect cell cycle progression. Genetic studies using *S. pombe* indicated that *chk1*$^+$ is essential for induction of the DNA damage-induced G2 checkpoint [12]. Additional biochemical studies revealed that induction of the DNA-damage checkpoint was associated with increase in the phosphorylation and amount of Wee1 in a Chk1-dependent manner [13]. Other genetic studies demonstrated that *chk1*$^+$ and *cds1*$^+$ are required for G2 checkpoint induction upon incompletion of DNA replication [14]. It was also shown that the DNA replication checkpoint was associated with Wee1 phosphorylation and that Cds1 could phosphorylate Wee1 in vitro [14]. These previous studies strongly suggest that in response to the signals generated by DNA damage or incomplete DNA replication, Wee1 is upregulated through Chk1/Cds1-dependent phosphorylation, which eventually results in the cell cycle G2 arrest.

rad24$^+$ was originally defined as a gene required for the cell cycle checkpoint mechanism following radiation-induced DNA damage in *S. pombe* [15]. The gene encodes a protein whose primary structure is homologous to that of 14-3-3 proteins of higher eukaryotes [15]. 14-3-3 proteins are a family of proteins that bind to a variety of cellular proteins mostly at their phosphorylated motifs and modify their subcellular localization and function. It is likely that Rad24 also regulates various cellular processes including the cell cycle control through similar mechanisms [16].

To further investigate the mechanism of Vpr-induced G2 arrest in this study, Vpr was expressed in *S. pombe* with various genetic backgrounds, and the effects on Wee1 expression were examined. Our data indicated that Vpr caused increase in the phosphorylation and amount of Wee1 associated with G2 arrest induction. Intriguingly, similar results were obtained when Vpr was expressed in the strains bearing *chk1* and *cds1* mutations. In *rad24* mutant, the level of Wee1 expression was low in the absence of Vpr, and even in the presence of Vpr, it was not increased as markedly as in the wild type (WT) strain. When certain subtypes of human 14-3-3 were expressed in *rad24* mutant, levels of Wee1 expression in the absence and presence of Vpr became comparable to those in WT, and the susceptibility to Vpr-induced G2 arrest was restored. The results of this study are compatible with the possibility that in fission yeast, Vpr could induce Wee1 phosphorylation through a novel mechanism in a Chk1- and Cds1-independent manner and that Rad24/14-3-3-dependent high-level expression of Wee1 might be necessary for Vpr-induced G2 arrest.

2. Materials and methods

2.1. Plasmid

Plasmid, pREP1-vpr, for expressing *vpr* gene of HIV-1_{NL4-3} [17] in a thiamine-repressible manner, was described previously [8]. To construct expression vectors for Vpr from HIV-1 clinical isolates, *vpr* gene fragments derived from isolates #16 and #17 [18] were obtained by PCR, cloned in pBluescript SK II(+) (Stratagene), and then subcloned in pREP-1 to construct pREP1-vpr16 and vpr17, respectively. Nucleotide sequences of these *vpr* clones were determined by the dideoxynucleotide chain termination method. For construction of 14-3-3 expression vectors, cDNA fragments of human 14-3-3 were prepared by RT–PCR using HeLa cell total RNA as a template. Upstream and downstream primers for PCR were 5′-AGAAGCAGGAAGAGCACTGG-3′ and 5′-GGACAGATCACAAAGCACGA-3′ for 14-3-3β, 5′-GGAGACACTATCCGCTTCCA-3′ and 5′-TGGTTTCTCTTGTTGGCTTATG-3′ for 14-3-3ε, and 5′-GGACTACGACGTCCCTCAAA-3′ and 5′-TGAGGCAGACAAAAGTTGGA-3′ for 14-3-3ζ. Amplified fragments were cloned in pT7-Blue (Novagen) and then subcloned in a *S. pombe* expression vector pAUR224 (Takara Bio), then the nucleotide sequences were verified.

2.2. Culture and transformation of S. pombe

Schizosaccharomyces pombe strains used in this study are listed in Table 1. *S. pombe* strain carrying a gene encoding Wee1 with an N-terminal HA_3-His_6 tag (HA-*wee1*$^+$) in place of the endogenous *wee1*$^+$ gene [13] was provided by M. O'Connell (Peter MacCallum Cancer Institute, Melbourne, Australia). Other mutant strains were originally obtained from Paul Nurse (ICRF, London, UK), Antony M. Carr (University of Sussex, Brighton, UK), and Mitsuhiro Yanagida (Kyoto University, Kyoto, Japan). Strains designated as "our stock" in Table 1 were generated in our laboratory by modifying their nutrition requirement properties through mating and tetrad analysis. Fission yeast cells were grown at 30 °C in the minimal medium (MM) supplemented with or without leucine (250 μg/ml), using standard culture techniques [19]. Transformation of *S. pombe* with plasmid DNA was carried out by the lithium acetate method as described [19]. For repression of the *nmt1* promoter, 10 μM of thiamine was added to the medium. To induce transcription from the *nmt1* promoter, cells were washed twice with MM without thiamine and then reinoculated into MM lacking thiamine. For selective growth of the cells transformed with pAUR224-based vectors, 0.5 μg/ml of aureobacidin A (Takara Bio) was added to the medium.

2.3. Cell cycle analysis

S. pombe cells in the mid-log growth phase were seeded in nitrogen-limited MM supplemented with or without thiamine at a density of 2×10^5/ml and grown at 30 °C for 36 h with vigorous shaking. Then the cells were fixed with 70% ethanol,